SPATIAL CONCENTRATIONS OF TRACE ELEMENTS IN KERATIN

by

Lihai Hu

A thesis submitted to the faculty of
The University of Utah
in partial fulfillment of the requirements for the degree of

Master of Science

in

Geology

Department of Geology and Geophysics

The University of Utah

May 2016

The University of Utah Graduate School

STATEMENT OF THESIS APPROVAL

The thesis of **Lihai Hu**

has been approved by the following supervisory committee members:

Diego P. Fernandez	, Chair	**09/02/2015** Date Approved
Thure E. Cerling	, Member	**09/08/2015** Date Approved
Brett James Tipple	, Member	**09/03/2015** Date Approved

and by **John M. Bartley**, Chair/Dean of

the Department/College/School of **Geology and Geophysics**

and by David B. Kieda, Dean of The Graduate School.

ABSTRACT

Bulk analysis of trace elements in hair can be unreliable because there are two sources of trace elements: (1) an endogenous source, which is physiologically incorporated into hair structure during hair growth; and (2) an exogenous source, which accumulates on the surface layer and may then diffuse into the hair interior. Here, I studied the spatial distribution and diffusive behavior of trace elements to understand these two sources. Concentration profiles of cross-sections of hair and horn for Al, Mg, Zn, and Mn were obtained by laser ablation analysis. Internal trace element concentrations in animal horns were used as reference values for the physiological level of trace elements in keratin. In addition, trace element concentrations in both abraded and unabraded segments from elephant and giraffe tail hair were measured. By comparing those measurements, eleven measured trace elements are classified into four groups: (1) insoluble group, Al and Ti; (2) physiological group, Cu, Zn, and Se; (3) alkaline earth group, Mg, Ca, Sr, and Ba; and (4) special group, Mn and Pb. As a case study, two sources of Sr with distinct isotopic compositions were identified in a horse tail hair, using sequential, longitudinal sampling, and mixing model analysis. The classification of trace elements and Sr isotopic analysis provide guidelines for future studies on trace elements in hair.

CONTENTS

LIST OF FIGURES

LIST OF TABLES

ACKNOWLEDGMENTS

I would like to express my gratitude to my advisor, Dr. Diego Fernandez, for his support, patience, and encouragement throughout my graduate studies.

My thanks also goes to my supervisory committee members, Dr. Thure Cerling and Dr. Brett Tipple, for reading the draft of this thesis and providing valuable suggestions and comments that improved this thesis.

I would also like to thank Christopher R. Anderson and all lab assistants in ICP-MS Metals Laboratory for giving technical support.

I would like to give my special thanks to Dr. Dean Troili, adjunct instructor in the School of Medicine and my former landlord, for the helpful discussion and suggestion on my research and the enormous help of grammar on my thesis editing.

Last, but not least, my deepest gratitude and love to my parents for their support, encouragement, and love throughout all my life.

CHAPTER 1

INTRODUCTION

> Geoscience tools and techniques, including the application of geochemical and isotope tracers and the evaluation of geomorphic and hydrologic processes, can provide insights into ecological processes. Likewise, ecological and microbial tools such as plant and microbial community characterization can provide insights into cycling of major and trace elements in the earth's crust. (Holloway, Ewing, & Maher, 2009)

Keratinized tissue (hair, nail, horn, feather, etc.) is a recorder of both dietary and environmental information, which can reveal geographical information; it is also a bio-monitor of exposure to environmental pollutants and can be used to study paleoclimatic change. Thus, hair and other keratinized tissue can be important to forensic studies, especially as related to geographic provenance or environmental contamination. Human hair is comprised of five major elements (hydrogen, oxygen, carbon, nitrogen, and sulfur), which compose about 99% of the total mass, and trace elements making up less than 1% of the total mass (Robbins, 1994). The composition of keratinized material is determined by the blood chemistry, which in turn depends on diet. Once keratinized material grows out of skin and is exposed to the environment, its chemical composition can be altered by the external contamination from particulates in the atmosphere and/or solutes and particles in water (Chittleborough, 1980; Kempson & Lombi, 2011).

The isotopic analyses of both major elements and trace elements in keratin have been utilized in dietary, geographical, and paleoclimatic studies. Cerling and Harris (1999) show a correlation between the carbon isotopic composition of keratin, hoof and hair, and diet in ungulate mammals. Sequential isotopic analyses of hairs have also shown that carbon- and nitrogen-isotope compositions can document dietary shifts in humans (Webb, White, & Longstaffe, 2013) and elephants (Cerling et al., 2006). Ehleringer et al. (2008) demonstrate that hydrogen- and oxygen-isotope compositions in human hair reflect the composition of drinking water, which can potentially reveal the individual's geographic history. Hobson and Wassenaar (1996) report a strong link of the hydrogen stable isotope between the breeding sites and the feathers of migrant songbirds. Iacumin, Davanzo, and Nikolaev (2006) report

that the geographical and temporal variation of carbon and nitrogen isotopic composition of mammoth hairs can be utilized as indicators of climate changes in the past. The isotopic analyses of the trace element strontium have been used to track human geographical movement (Font et al., 2012) and bird migration (Font, Nowell, Graham Pearson, Ottley, & Willis, 2007).

The analyses of trace elements in hair have been utilized as monitors of dietary change and exposure to pollutants in certain environmental settings. Bio-monitoring studies of toxic metals in human hair show that the intake history of mercury and selenium can be reconstructed by sequential human hair analysis (Gellein et al., 2008; Yoshinaga, Shibata, & Morita, 1993). Nowak and Chmielnicka (2000) found that the lead concentration in human hair was a marker to environmental pollution of lead. Lin et al. (1999) concluded that cadmium, lead, and copper concentrations in human hair reflected the status of environmental pollution. Patra et al. (2007) showed that high lead concentration in cow tail hair was an indicator of blood lead concentration in cattle. The combined concentration and isotopic analyses of lead in human hair reveal that the primary source of the body lead for people living in Mitrovica, northern Kosovo, is from the nearby Zveçan smelter, probably through the ingestion and/or inhalation of Pb-contaminated soils and house dust (Brewer, Bird, & Macklin, 2016).

Despite the wide use of keratin in biological, geographical, and environmental applications, the reliability of elemental analyses of keratin is still arguable due to lack of understanding in the effect of the exogenous contribution of elements. For the five major elements, the exogenous contribution is negligible compared to the endogenous signal, thus the isotopic compositions of these elements in keratin do not change with environmental exposure. However, the concentrations and isotope ratios of trace elements can change due to environmental exposure. A clear identification of endogenous and exogenous signals in keratin would provide valuable information for the link between mammal behavior and the geochemical contribution from the environment. Therefore, an effective procedure to separate the exogenous signal from the endogenous signal is critical to the study of physiological and contaminating processes that affect the abundance of trace elements in keratin. Many hair studies assume the washing methods adopted could quantitatively separate the exogenous signal from the keratin while not changing the endogenous signal for all studied trace elements. However, the effectiveness and reliability of these decontamination procedures are questionable due to the lack of chemical knowledge of binding sites and migrating behaviors of trace elements in hair (Barbosa Jr, Tanus-Santos, Gerlach, &

Parsons, 2006; Chittleborough, 1980; Kempson & Skinner, 2012). Thus, the applications of the analysis of trace elements in hair are limited to a few trace elements (Kempson & Lombi, 2011).

To study the influence of exogenous contribution to the concentrations of trace elements in keratin, a reference level of the endogenous component of trace elements in keratin is needed. In this thesis, I established a *reference of endogenous levels of trace elements of keratin* from the interior of animal horn for comparison with external contamination. Animal horns are made of the same keratin as hair (Block, 1951), so similar physiological growth process should incorporate similar amounts of trace elements into the hair structure. Because of the large radius of horns compared to hairs, the interior of horn has a lower exogenous component of trace elements than does hair. The environmental contamination in the outer part of horn are mechanically removed using a rotary tool in this study. The analysis of a set of horn interiors provides ranges of trace element concentrations, representing the likely endogenous intervals of trace elements in keratin.

I studied the distributions and behaviors of trace elements in horn and hair by comparing their endogenous intervals with the bulk and internal concentrations, using in-situ laser ablation and chemical analysis. To eliminate problems found during chemical cleaning (Kempson & Skinner, 2012), the surface layer was manually abraded to remove external contamination. Elephant and giraffe tail hairs were used in this study because they share the same structure—cuticle, cortex, and medulla (Hausman, 1920; Yates, Espinoza, & Baker, 2010)—with human hair while their wider diameters ($\sim$1 mm and $\sim$0.6 mm, respectively) allow mechanical abrasion in contrast with human hair ($\sim$0.1 mm). Four groups for the measured trace elements were recognized according to their spatial distributions and chemical behaviors: (1) insoluble group (2) physiological group (3) alkaline earth group, and (4) special group. Distributions and behaviors of trace elements in keratin will help design measurement strategies to target questions related to either intake or external contamination and will help recognize meaningful interpretations of trace elemental analysis in hair. As a case study, sequential Sr isotopic analysis on a strand of horse tail hair was conducted to identify the sources of Sr in horse tail hair. Using elemental and isotopic analyses of Sr for those segments, the mixing model from Faure and Mensing (2005) resolves the two distinct sources of Sr in the horse tail hair. This method can be applied to future human hair analyses for forensic and environmental studies.

CHAPTER 2

SAMPLES AND METHODS

2.1 Samples

Five horn tips were collected from several species of African animals (Kongoni, Wildebeest, Bushbuck) at a commercial game ranch in Kenya. One complete bison horn was collected from a bison on Antelope Island, Utah, USA. Elephant tail hairs and giraffe tail hairs were provided by the Kenya Wildlife Service. Horse tail hairs were collected from a stable in Utah. Only two strands of elephant hair, one strand of giraffe hair, and one strand of horse hair were utilized in this study.

2.2 Instrumentation and sample handling

Instruments used in this thesis were all at the ICP-MS Metals Lab in the Department of Geology and Geophysics at the University of Utah. Laser ablation was performed using Analyte G1 excimer laser ablation system (Photon Machines Inc.; Bozeman, MT, USA). Sample digestion was performed using the ETHOS EZ microwave digestion system (Milestone Inc.; Shelton, CT, USA). Concentration measurements for both laser ablation and digestion were performed using the Agilent 7500ce inductively coupled plasma quadrupole-mass spectrometer, ICP-Q-MS, (Agilent Technologies, Inc.; Santa Clara, CA, USA).

Prior to chemical digestion or plug mounting, all samples were cleaned in an ultrasonic bath with ethanol and Milli-Q water sequentially, and then air-dried overnight in a laminar flow hood at room temperature. Before sample mounting for laser ablation, acrylic cylindrical plugs were cleaned in an ultrasonic bath with FL70 detergent and Milli-Q water sequentially, then air-dried overnight in a laminar flow hood at room temperature. After mounting the samples with epoxy, the plugs were put in a 60 °C oven for four hours to accelerate the solidification process, and then cooled to room temperature. The plugs were sequentially polished using 30, 9, and 3 µm grade 3M™ Wetordry™ sandpapers, cleaned in an ultrasonic bath with Milli-Q water to remove any possible contaminants from the

sandpapers, then air-dried overnight in a laminar flow hood at room temperature.

Longitudinal distances in this thesis refer to the distance of sample from the root of the hair. Proximal end refers to the root of the hair and distal end refers to the tip of the hair.

2.3 Project 1: Trace elements in keratin

To understand the spatial distribution and the behaviors of trace elements in keratinized structures, the following experiments were performed.

2.3.1 Surface abrasion of hairs

The external surface of a single elephant and a single giraffe hair was removed by abrasion to remove surface contaminants. A single elephant tail hair and a single giraffe tail hair were partially covered by Scotch® Box Sealing Tape. Segments a, c, e, and g of these two hairs were left uncovered for abrasion (Figure 2.1). The outermost parts of segments a, c, e, and g were then abraded using 3M™ Stikit™ Gold 216U sandpaper, P240 grit (Figure 2.2). The tape was then removed and the residual adhesive on the hairs was wiped away with 190 proof ethanol (Decon Laboratories, Inc.; King of Prussia, PA, USA). Segments a, b, c, d, e, f, and g were then manually cut using a razor blade. They were cleaned and dried as described in section 2.2 before chemical digestion. In this procedure, the outer 40 to 130 µm of the hair was removed by abrasion; the lengths and the diameters of hair segments before and after abrading procedure are reported in Table 2.1.

2.3.2 Laser ablation on cross sections of elephant and giraffe hair

One 2 mm unabraded segment of each hair sample was cut from segment d (Figure 2.1) and mounted vertically with epoxy in 1 mm (diameter) × 1 mm (depth) cylindrical wells drilled in an acrylic cylindrical plug. Laser-ablation line analyses passing through the medulla of the hair on two hair cross sections (Figure 2.1) were performed. The laser system used a 14.5-µm circular beam with 10 Hz firing frequency moving at 4 µm/s. The

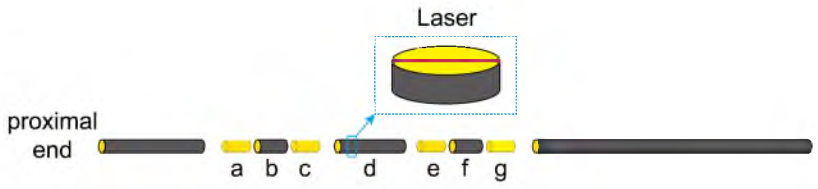

Figure 2.1: Schematic diagram of the sampling method for the elephant and the giraffe hair. The surface of segments a, c, e and g was removed by abrasion with sandpaper. One part of segment d was cut for laser ablation analysis. The red line on the cross section represents the laser path.

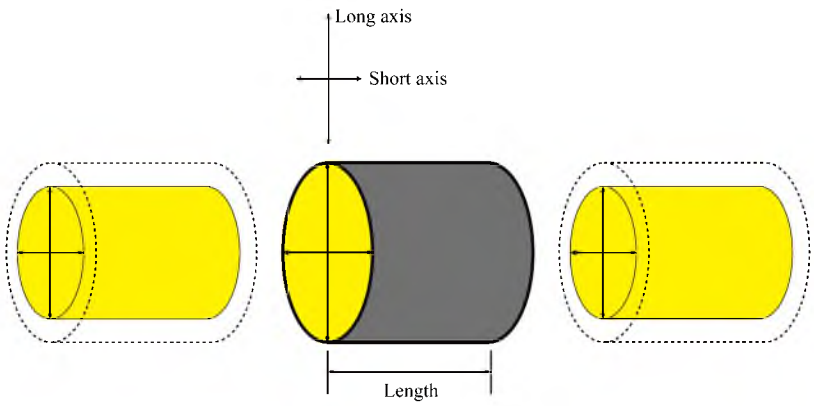

Figure 2.2: Schematic diagram showing the diameters of one unabraded hair segment and two abraded hair segments reported in Table 2.1.

Table 2.1: Lengths and diameters of the hair segments before and after abrasion (the unit of all numbers is mm).

Segment	Longitudinal	Segment	Before abrasion		After abration	
number	distance	length	Long axis	Short axis	Long axis	Short axis
Elephant hair						
EH-a	46	19	0.90	0.54	0.76	0.42
EH-b	67	21				
EH-c	91	23	0.88	0.52	0.62	0.44
EH-d	117	48				
EH-e	165	19	0.74	0.54	0.49	0.41
EH-f	187	22				
EH-g	212	20	0.71	0.53	0.46	0.40
Giraffe hair						
GH-a	41	37	0.68	0.64	0.56	0.48
GH-b	82	38				
GH-c	122	31	0.66	0.59	0.55	0.47
GH-d	157	20				
GH-e	177	34	0.62	0.47	0.45	0.33
GH-f	216	33				
GH-g	251	34	0.62	0.44	0.53	0.34

ablated material was transported online to the Agilent 7500ce ICP-Q-MS, which measured the signal intensity of $^{24}Mg^{+}$, $^{27}Al^{+}$, $^{55}Mn^{+}$, and $^{66}Zn^{+}$. Five-point averaging was applied to the raw intensity data. Due to the lack of an internal reference element for hair analysis, the estimated concentrations of Al, Mg, Zn, and manganese (Mn) were calculated by normalizing the signal intensity of these ions to the external standard, NIST 610 – glass certified reference material, after background correction. The detection limits of Al, Mg,

Zn, and Mn were about 50 mg/kg, 30 mg/kg, 15 mg/kg, and 20 mg/kg, respectively.

2.3.3 Surface removal of horns

To study uncontaminated keratin tissue, surfaces of horn samples were removed. The surfaces of all six horn tips were removed using a Dremel® 8100 8V Max rotary tool with a circular carbide saw blade. About half the weight, including the surface, was removed for each horn tip. The final weights of the prepared horn tip interiors were about 50 mg. The complete bison horn was cut longitudinally into two pieces. Two rectangular segments laterally perpendicular to the surface were cut from one of the halves (Figure 2.3) using an IsoMet® cutting tool with isopropanol as cooling fluid. One rectangular segment with surface layer was cleaned and dried for laser ablation analysis. The other segment, with the surface layer removed, was cut with the IsoMet® cutting tool into ~ 0.3 cm × 0.8 cm × 0.3 cm bars (~50 mg) from the medulla to sub-surface. These horn interior bars were polished using 30 µm grade 3M™ Wetordry™ sandpaper. Then they were cleaned and dried as described in section 2.2 before chemical digestion.

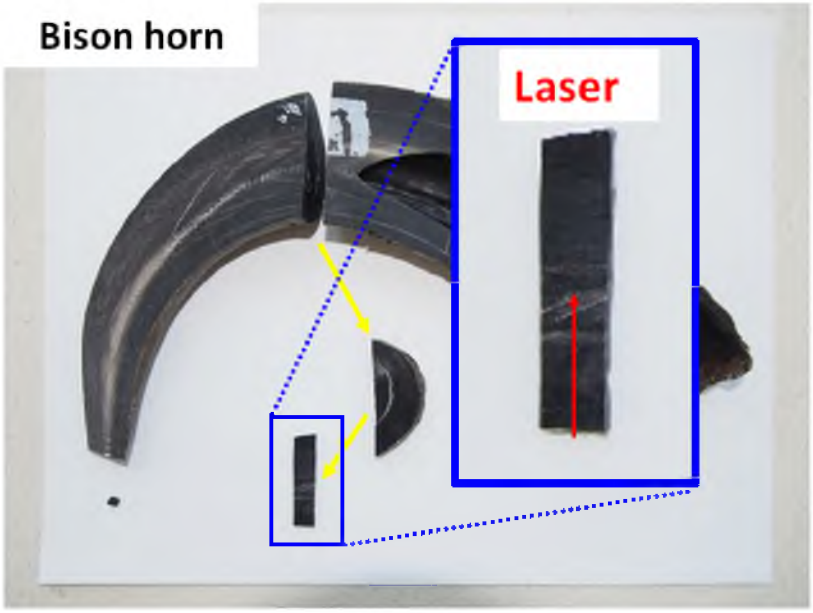

Figure 2.3: Bison horn sampling. The rectangular segment shown here is the segment for laser analysis. There is another rectangular segment that was cut into bars for chemical analysis. In the bottom left corner of the figure is the horn interior of which the surface layer has been removed. The paper beneath the samples is letter-size (8.5 × 11 inches).

2.3.4 Laser ablation on a transverse section of the bison horn

One ~0.3 cm × 0.8 cm × 1 cm rectangular segment of bison horn with an intact surface was mounted horizontally with epoxy in a 5 mm-deep groove drilled in an acrylic cylindrical plug. Laser-ablation line analysis passing the surface layer was performed (Figure 2.3). The laser system used 86.2-µm square beam with 10 Hz firing frequency moving at 10 µm/s. The ablated material was transported online to Agilent 7500ce, which measured the signal intensity of $^{24}Mg^{+}$, $^{27}Al^{+}$, $^{55}Mn^{+}$ and $^{66}Zn^{+}$ as above. The detection limits of Al, Mg, Zn and Mn were about 0.5 mg/kg, 0.8 mg/kg, 0.4 mg/kg and 0.3 mg/kg, respectively.

2.4 Project 2: Al-enriched surface layer

This project included two detailed studies of the properties of the Al-enriched surface layer of elephant hair using laser ablation in-situ analysis.

2.4.1 Laser ablation on cross sections of elephant hair

One strand of elephant hair with an intact cuticle was chosen to study changes in elemental concentration with distance from hair root. This hair was manually cut with a razor blade into ~2 mm-long segments from the longitudinal distance of 12.3 mm to 124.0 mm (Figure 2.4). These segments were cleaned and dried prior to mounting. Clean segments were then mounted vertically with epoxy in 1 mm (diameter) × 1 mm (depth) cylindrical wells drilled in an acrylic cylindrical plug. The laser-ablation line analyses from the center outwards on every cross section were then performed (Figure 2.4). The laser system used a 31.4-µm circular beam with 10 Hz firing frequency at 3 µm/s or 4 µm/s moving velocity. The ablated material was transported online to the Agilent 7500ce, which measured the signal intensity of $^{27}Al^{+}$ and $^{56}Fe^{+}$ as before. The detection limits of Al and Fe were about 20 mg/kg and 10 mg/kg, respectively.

2.4.2 Multiple laser ablation on one cross section

The cross section at the longitudinal distance of 76.3 mm was chosen from the elephant hair in the last experiment to study the homogeneity of the surface layer of elephant hair. The laser system used a 31.4-µm circular beam with 10 Hz firing frequency at 2 µm/s moving velocity. The ablated material was transported online to Agilent 7500ce, which measured the signal intensity of $^{27}Al^{+}$ as before. Twenty-six laser ablation line analyses perpendicular to the periphery of the hair were performed on this cross section (Figure 2.5). All of these lines passed the surface layer of the hair. The detection limit of Al was about 100 mg/kg.

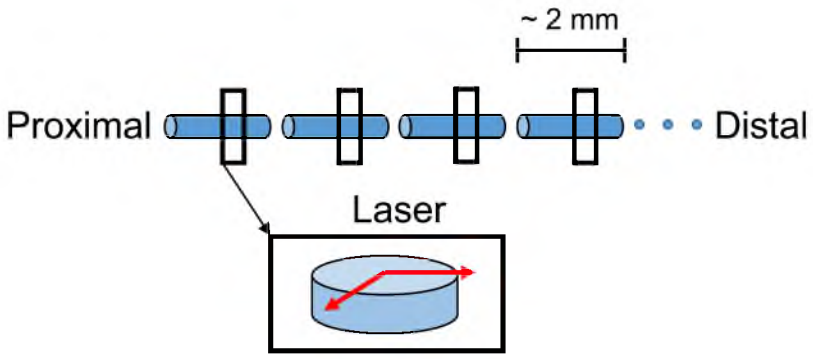

Figure 2.4: Schematic diagram of the sampling method for elephant hair laser ablation analysis. The elephant hair was cut into 2 mm segments and the cross section in the middle of each segment was analyzed. The red arrows on the hair cross section represent the laser path.

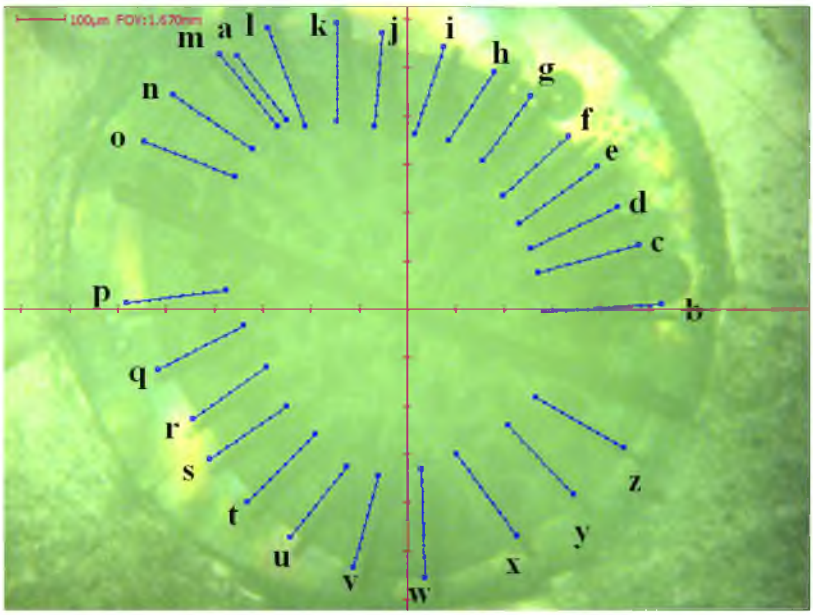

Figure 2.5: Photo of the cross section of the elephant hair at distance of 76.3 mm from proximal end. Blue tracks with letters represent 7.2-µm laser-ablation paths.

2.5 Project 3: Source partitioning of Sr in horse hair

To differentiate the signals of mixed sources of Sr in hair, one strand of horse tail hair was chosen in this project. Sr isotopic analysis was applied to hair segments sequentially cut from this strand of horse tail hair.

2.5.1 Horse hair sequential sampling

One single horse tail hair, ~60 cm long, was wiped with 190 proof ethanol and Milli-Q water, respectively, to remove the possible surface contamination residue, and was dried

using Ar gas.

This hair was manually cut with a razor blade into 20 segments. Segments were ~3 cm long with the exception of the four most distal segments from the hair root, which were ~4 cm long. The longer length for these four most distal segments was to compensate for the mass loss due to abrasion (smaller diameter). Ten alternate segments were picked for concentration and isotopic analyses (Figure 2.6).

2.5.2 Sr purification and isotopic analysis

The off-line chromatography method was adopted for Sr purification. Twenty columns were made from Zeus® polytetrafluoroethylene (PTFE) heat shrink tube (4:1). The tube was cut into 4 cm lengths and sheathed on a 3/8-inch internal diameter (I.D.) Teflon® rod. The tube-rod assembly was heated with an air gun to > 350 °C. After shrinking and recovering to the column shape, the tube was quenched in liquid nitrogen for fast solidification. A frit, made from 70 µm porous polyethylene sheets (Scientific Commodities Inc.; Lake Havasu City, AZ, USA), was installed in the column. Final resin volume of the column was about 50 µL with an aspect ratio of four and a 1 mL reservoir volume. These columns were cleaned in aqua regia overnight and were then rinsed with Milli-Q water before use. The 100-150 µm Sr Resin produced by Eichrom® Technologies, LLC was used in this study. The 50 µL resin was sequentially cleaned with 8M HNO_3 and Milli-Q water. Then 4 × 0.25 mL 8M HNO_3 were loaded to condition the column. A sample solution of concentrated HNO_3 from the digestion process was then loaded onto the column. The resin was rinsed by another 4 × 0.25 mL 8M HNO_3 step. Strontium was recovered by 4 × 0.25 mL Milli-Q water. The eluted solution containing Sr was then dried and dissolved in 2.4% HNO_3 for Sr isotopic measurement.

All isotope ratios were measured using a Thermo Neptune Multi-collector ICP-MS at the ICP-MS Metals Lab. A quartz dual cyclonic spray chamber with a perfluoroalkoxy alkane (PFA) nebulizer, a 20 µL/min self-aspiration capillary probe, a quartz torch and nickel cones were used. Masses 83, 84, 85, 86, 87, 88 were simultaneously measured in L4, L3, L2,

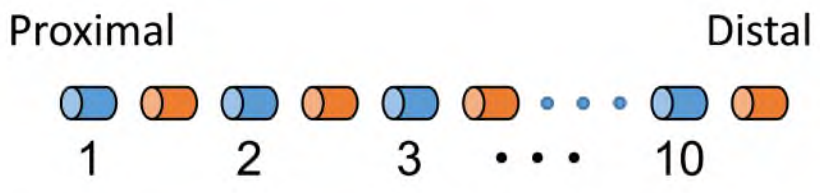

Figure 2.6: Schematic diagram of the sampling method for the horse tail hair. The hair was cut into twenty 3-cm segments and segments 1 to 10 were digested and analyzed.

L1, C, H1 and H2 faraday cups, respectively. ^{84}Kr and ^{86}Kr interferences on ^{84}Sr and ^{86}Sr, respectively, were corrected by subtracting the amount of ^{84}Kr and ^{86}Kr corresponding to the ^{83}Kr signal with a standard isotopic composition (Böhlke et al., 2005). ^{87}Rb interference on ^{87}Sr was corrected by subtracting the amount of ^{87}Rb corresponding to the ^{85}Rb signal with a standard isotopic composition (Böhlke et al., 2005). ^{88}Sr signal was about 0.5 V for a 10 ppb SRM 987 solution. Each analysis consisted of 170 ratio measurements with a one-second integration time. Instrumental and analytical mass fractionations were corrected for each $^{87}Sr/^{86}Sr$ ratio by normalizing to $^{88}Sr/^{86}Sr = 8.375209$ using the exponential law. After mass-bias correction, outlier ratios in each measurement (outside of two standard deviations of all normal ratios) were discarded. The average corrected $^{87}Sr/^{86}Sr$ ratio of each measurement was reported as the Sr isotopic composition of each sample. SRM 987 reference material with 10 ppb concentration was run between every two samples to check the machine status. The Sr concentrations in the sample solutions varied from 10 ppb to 30 ppb. The uncertainty of sample measurements was set to ± 0.0002 (2SD) based on the daily reproducibility of ± 0.00024 (2SD) of the 10 ppb SRM 987. The daily $^{87}Sr/^{86}Sr$ average of SRM 987 standard was 0.71029 ± 0.00024 (2SD).

2.6 Microwave digestion method

Thirteen horn interiors (~50 mg), six elephant hair segments (~50 mg), six giraffe hair segments (~10 mg) and ten horse tail hair segments (~1.5 mg) from those projects (section 2.3 and section 2.5) were digested in Teflon® vessels with a mixture of 2 mL HNO_3 and 0.25 mL H_2O_2 using Milestone ETHOS EZ microwave digestion system, following Tipple, Chau, Chesson, Fernandez, and Ehleringer (2013). A 0.1 mL aliquot of the total ~2 mL digest from each sample was transferred to a 15 mL tube and brought up to 10 mL for chemical abundance analysis. A 0.2 mL aliquot of the total 2 mL digest of each horse hair sample was transferred into a 15 mL tube and brought up to 4 mL, due to their low mass, for chemical abundance analysis. All dilutions were done gravimetrically.

2.7 Chemical concentration analysis

The abundances of eleven trace elements (Mg, Al, Ca, Ti, Mn, Cu, Zn, Se, Sr, Ba and Pb) were measured for all microwave-digested samples, except the horse hair segments of which only Sr concentration was measured. A quartz dual cyclonic spray chamber with a perfluoroalkoxy alkane (PFA) nebulizer (0.1 mL/min), a quartz torch, and platinum cones were used. Indium was added to all samples as an internal calibration standard at the concentration of 50 µg/kg. Standard reference solutions T-205 (USGS, Reston, VA,

USA) and SRM 1643e (NIST, Gaithersburg, MD, USA) were measured as consistency standard and reference material, respectively, during each analytical run. The long-term reproducibility for T-205 and differences relative to the accepted values suggested the uncertainty of concentration measurement was less than 10%.

2.8 Contamination test

In order to test for possible contamination from cutting and surface-removing procedures, the following experiment was done. One 3/16 inch-wide PTFE rod was soaked in aqua regia for two days, rinsed with Milli-Q water and then dried in a laminar flow hood. This rod was cut into about 0.5 mm-thick thin sections by three methods: manual cutting with razor blade, slow cutting with IsoMet® low speed saw and fast cutting with Dremel® 8100 rotary tool with a circular diamond-coated blade. All pieces were cleaned separately in an ultrasonic bath with ethanol and Milli-Q water, respectively, and dried in a laminar flow hood. The pieces, cut by the same method, were then divided into three or four groups of different sizes: one piece, two pieces, three pieces and four pieces (only for the razor-cutting) (Figure 2.7). All ten groups with PTFE rod pieces were then processed through the same microwave digestion procedure as samples and the concentrations of trace elements were measured with the Agilent 7500ce following the same procedure as used for the samples.

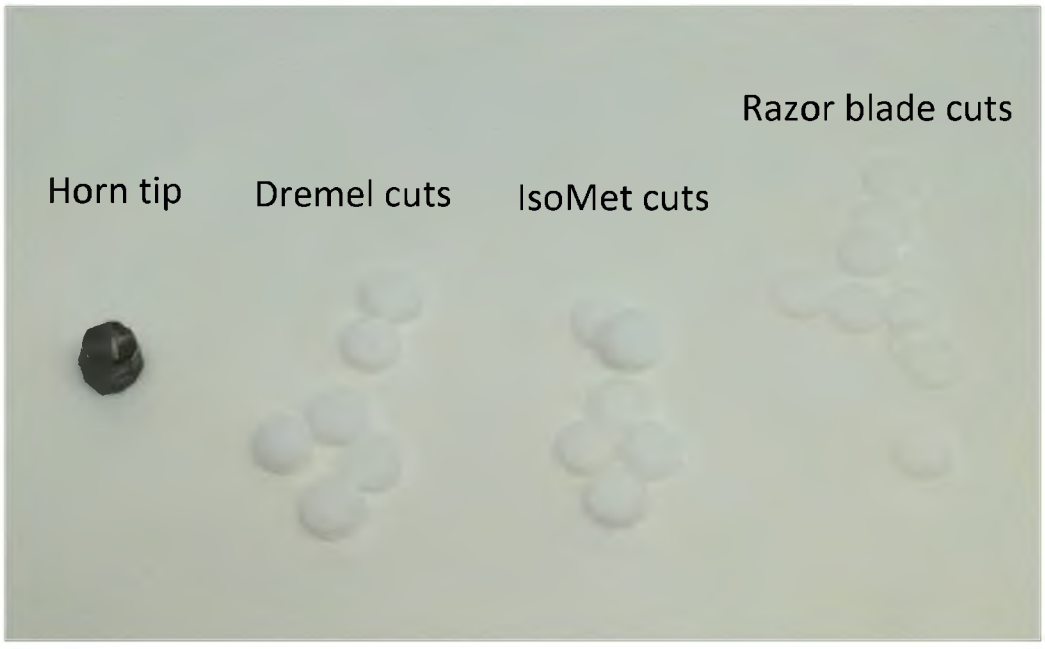

Figure 2.7: After-cutting horn tip sample and after-cutting cuts in contamination test using PTFE. The diameter of the PTFE cuts is 3/16 inch.

CHAPTER 3

RESULTS

3.1 Laser ablation of elephant and giraffe hair cross sections

Profiles of estimated concentrations of Al, Mg, Zn and Mn in the cross sections of elephant and giraffe hair were obtained using laser ablation in-situ analysis (Figure 3.1). These elements showed distinct patterns of variation. Although Al, Mg and Mn were relatively enriched in the surface layer, the internal spatial distribution of each element was different from the others. Zn was depleted in the surface compared to the core.

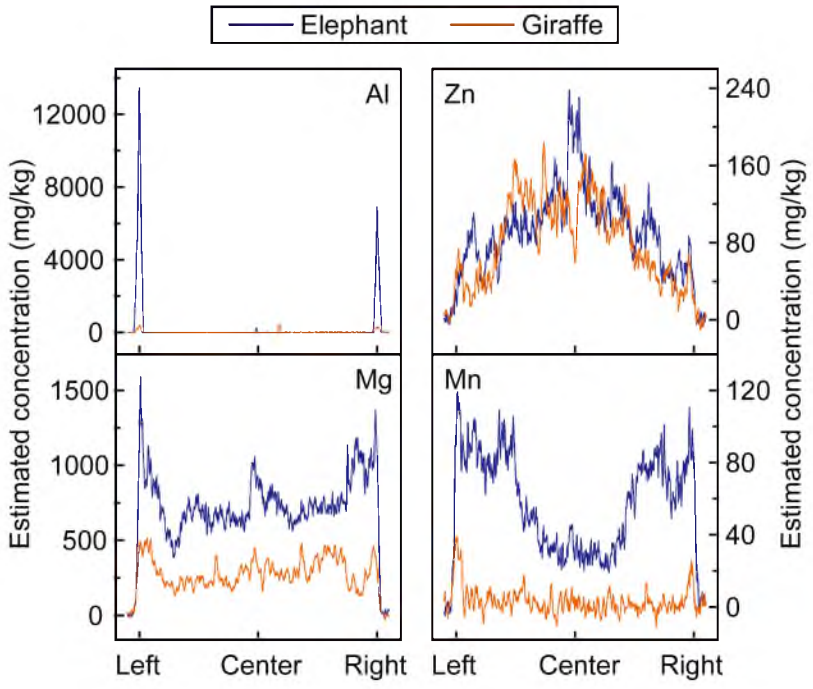

Figure 3.1: Laser profile of Mg, Al, Zn and Mn on the cross sections of the elephant hair and the giraffe hair. The horizontal scale is normalized. The true width of the elephant hair and the giraffe hair is 0.70 mm and 0.45 mm, respectively. The cross sections on the elephant hair and the giraffe hair are about 13 cm and 17 cm from proximal end, respectively.

Al was extremely enriched in the surface layer of elephant hair compared to the core: the intensity in the surface was more than three orders of magnitude larger than the interior. The Al intensity differed between the two sides of the hair crossed by the laser transect, indicating the spatial distribution of Al in the surface layer of elephant was not homogeneous. Al intensity of the internal part of the elephant hair was generally below detection limit, except for some minor peaks near the center. Giraffe hair also had enriched Al in the surface layer, although the intensity was much lower than elephant hair. The peak intensity in the giraffe hair surface layer was comparable to the peak near the center. The relatively small (~100 mg/kg) peaks near the center found in both elephant and giraffe hair could be small fragments from the ablated area or real signals measured in the hair interior, suggesting small scale Al binding sites in the internal structure of the hairs. For giraffe hair, the internal peak intensity was comparable to the surface content; for elephant hair, the internal peak intensity was negligible compared with surface content.

Elephant hair had high Mg concentrations in the surface layer, showing a sharp peak similar to Al. Although less enriched than Al, Mg intensity in the surface layer was about twice the intensity of Mg in the interior of the elephant hair. The giraffe hair did not show sharp enriched peaks on the surface layer but had a relatively enriched wider peak near the hair surface. The elephant hair had higher Mg intensity than the giraffe in both the surface layer and the internal part. The enriched surface layer of elephant hair indicated an external contamination of Mg on the surface layer. Unlike Al, the internal part of both elephant and giraffe had a significant amount of Mg, suggesting partial-endogenous origin of Mg in the internal hair structure.

Elephant and giraffe hair had similar spatial distributions and comparable concentrations for Zn, with a higher concentration in the center and a lower concentration in the periphery. No enriched surface layer for Zn for either the elephant hair or the giraffe hair was observed.

The profile pattern of Mn observed for elephant hair was different from the giraffe sample. Mn in elephant hair had a relatively enriched surface layer with lower concentration in the core. The outer part of the elephant hair, possibly including regions within the cortex, had a much higher intensity than in the center—the medulla region. Therefore, even if the surface layer is excluded, different parts of the interior of the hair have distinct trace element concentrations. Although there was also a Mn-enriched surface layer in giraffe hair, Mn in internal part of giraffe hair was so low that it is difficult to determine whether there was the same variability as in the elephant hair or not.

3.2 Laser ablation near the surface layer on bison horn cross section

Profiles of estimated concentrations of Al, Mg, Zn and Mn on the cross sections of bison horn near the surface layer were obtained using laser ablation in-situ analysis (Figure 3.2). Al, Mg and Mn were extremely enriched in the surface layer of bison horn, indicating an external contamination within 1 mm of the surface. Al intensity in the surface layer was more than four orders of magnitude higher than internal intensity. Small Al peaks in the internal part of bison horn were also observed, indicating an endogenous portion of Al in the horn interior, although relatively low compared to the surface layer. Both Mg and Mn had small peaks inside near the surface layer. Mg internal intensity was clearly detectable while Mn internal intensity was close to the detection limit. Zn was not enriched in the surface layer compared to its substantial internal intensity. Although fluctuating, the Zn intensity from $\sim$4 mm inward was stable, while the Zn intensity decreases from $\sim$4 mm towards the surface layer.

3.3 Cutting method contamination test

Contamination may arise from cutting operations using metal blades for sectioning horn and hair or removing the surface of horns. A PTFE rod, used as a proxy for keratin, was cut using different methods. By comparing samples with increasing number of cuts, a possible link between cutting and contamination was evaluated.

Unlike the abrasion of individual hair strands using sand paper, the methods for cutting horn and the removal of its surface layer used metal circular blades and metal razor blades, which raised the question of possible contamination. A contamination test for all three cutting methods provided the answer. The result is shown in Table 3.1. Sample ID wheel represents samples cut with a Dremel® 8100 rotary tool with a circular blade. Sample ID IsoMet represents samples cut with an IsoMet® low speed saw. Sample ID Razor represents samples manually cut with a razor blade.

The concentration of Ca and Mn in the final digestion solution was below or close to the method detection limit, so these two elements had no measurable contamination from either cutting method or the chemical digestion process. The concentration of other elements in the final digest was detectable and resolvable by the analytical method. However, there was no obvious correlation between elemental concentration in the final digest and the number of cuts in the digestion vessel, suggesting that such detectable signal was not from the cutting methods but from the chemical blank of the entire sample processing procedure. The chemical blank was negligible though, compared to the concentration of trace elements

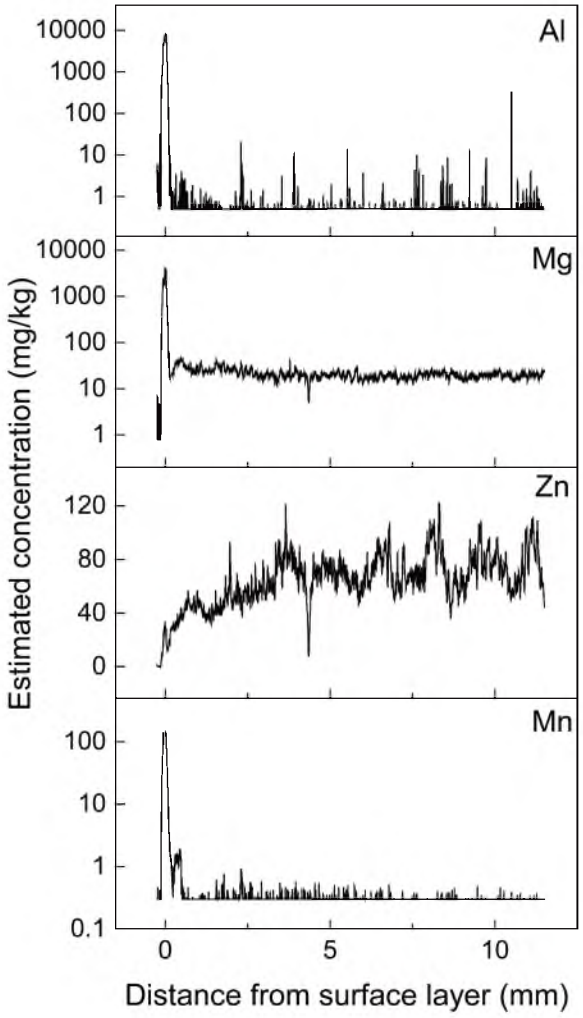

Figure 3.2: Laser profiles of Al, Mg, Zn and Mn on the transect of the bison horn crossing the surface layer. Positive distance represents the distance from surface layer inward, while negative distance represents reverse direction. The scales for Al, Mg and Mn are logarithmic.

in hair or horn samples. For instance, 50 mg (the amount that was digested) of a clean horn sample contained about 50 ng of Sr (∼1 mg/kg), which was 250 times more than the maximum amount of detectable Sr found in this test (IsoMet-2).

Only one measurement (IsoMet-2) had significantly high Cu contamination (41 ng Cu) compared to ∼350 ng Cu in horn samples (∼7 mg/kg Cu in ∼50 mg sample). Cu content in the other two samples (IsoMet-1 and IsoMet-3) were much lower than Isomet-2, although still higher than the samples cut by the other two methods. This Cu contamination was likely from the base material of the circular saw blade, which is made of brass. However, considering these three IsoMet samples did not have any correlation between Cu concentration and the number of cuts, such contamination must have resulted from a random

Table 3.1: Weight of elements (µg) in solutions after microwave digestion in the contamination test. Detection limit is the machine detection limit of the Agilent 7500ce in this experiment.

Sample ID	Mg	Al	Ca	Ti	Mn	Cu	Zn	Se	Sr	Ba	Pb
Detection limit	0.001	0.003	0.23	0.001	0.0007	0.001	0.0002	0.0003	0.00002	0.00004	0.00002
Wheel-1	0.005	0.104	<0.23	0.006	0.0007	0.002	0.0007	<0.0003	0.00005	0.00026	0.00017
Wheel-2	0.006	0.041	<0.23	0.002	<0.0007	0.001	0.0020	<0.0003	0.00005	0.00007	0.00016
Wheel-3	0.011	0.185	<0.23	0.007	0.0008	0.003	0.0023	<0.0003	0.00014	0.00082	0.00044
IsoMet-1	0.007	0.130	<0.23	0.007	0.0007	0.006	0.0009	<0.0003	0.00013	0.00144	0.00021
IsoMet-2	0.009	0.108	<0.23	0.003	0.0007	0.041	0.0016	<0.0003	0.00020	0.00076	0.00028
IsoMet-3	0.008	0.068	<0.23	0.003	<0.0007	0.008	0.0014	<0.0003	0.00018	0.00029	0.00023
Razor-1	0.004	0.041	<0.23	0.001	<0.0007	<0.001	<0.0002	<0.0003	0.00003	0.00011	<0.00002
Razor-2	0.005	0.145	0.29	0.007	<0.0007	0.003	0.0040	<0.0003	0.00012	0.00060	0.00007
Razor-3	0.019	0.082	<0.23	0.002	<0.0007	0.002	<0.0002	<0.0003	0.00017	0.00039	0.00008
Razor-4	0.006	0.099	<0.23	0.003	<0.0007	0.002	0.0007	<0.0003	0.00105	0.00004	0.00006
Digestion Blank	0.003	0.030	<0.23	0.001	<0.0007	0.002	<0.0002	<0.0003	0.00005	<0.00004	<0.00002

event. Unlike the samples cut from the PTFE rod, the bison horn interior samples cut by the IsoMet method were further abraded after IsoMet cutting, which should have removed the possible cutting contamination. Cu concentration measurements in bison horn interior samples, however, should still be treated with caution.

This contamination experiment for cutting methods confirmed that the surface-removal and cutting methods used in this study caused negligible contamination of trace elements in the samples considered.

3.4 Trace elements in horn interiors

The concentrations of eleven elements in thirteen horn interior samples were measured and reported in Table 3.2. The most abundant trace element was Ca, which had a range of 437–1110 mg/kg. There were two other elements, Zn and Mg, with concentrations higher than 10 mg/kg, while the concentrations of other elements were less than 10 mg/kg. Pb and Mn had the lowest concentrations, 0.02–0.27 mg/kg and 0.07–0.22 mg/kg, respectively. The variations of concentrations of all eleven elements were smaller than a factor of five except for the variation of Pb concentration, which was as large as 17 times (0.02–0.27 mg/kg). Thirteen samples could be divided into two groups: low Pb group which included the horn samples from African animals (0.02–0.07 mg/kg) and high Pb group which included only the Utah bison horn samples (0.06–0.27 mg/kg). The variations of Cu and Zn concentrations were smaller than a factor of two, 1.8 (5.2–9.2 mg/kg) and 1.6 (131–215 mg/kg), respectively.

3.5 Trace elements in hair segments

The concentrations of eleven elements in twelve hair segments (six from the elephant hair and six from the giraffe hair) were measured and reported in Table 3.3. There were four abraded segments of which the surface layer was removed and two unabraded segments between the abraded segments for each hair (Figure 2.1). All elements had higher concentrations in unabraded elephant hair segments than in unabraded giraffe hair segments, except for Se. The concentration differences of trace elements between abraded and unabraded segments in giraffe hair were relatively small except for Mn and Pb. The concentration differences of trace elements between abraded and unabraded segments in elephant hair were relatively large, especially Al and Ti of which the concentrations in abraded segments were more than one order of magnitude lower than the concentrations in unabraded segments.

Table 3.2: Concentrations of trace elements in the horn samples. The unit of the elemental concentrations is mg/kg.

Sample	Note	Weight (mg)	Mg	Al	Ca	Ti	Mn	Cu	Zn	Se	Sr	Ba	Pb
Bison horn interior													
BH4-1	Center	47	54	5.7	771	0.8	0.11	5.9	193	0.3	0.8	0.5	0.21
BH4-3		46	49	9.0	1110	1.2	0.13	6.3	198	0.3	1.1	0.6	0.24
BH4-4		52	46	8.6	1020	1.0	0.13	5.6	210	0.3	1.0	0.6	0.27
BH4-5		57	37	3.7	891	0.8	0.12	6.0	215	0.2	0.9	0.5	0.22
BH4-6	crack	61	25	4.1	519	0.4	0.08	6.0	194	0.2	0.5	0.3	0.14
BH4-7	crack	46	21	2.8	437	0.3	0.07	5.9	171	0.2	0.5	0.3	0.10
BH4-8	Near surface	57	30	3.3	604	0.5	0.07	5.2	153	0.3	0.6	0.8	0.06
Horn tips (interior)													
BH5	Bison	56	42	4.6	550	0.5	0.14	6.2	187	0.5	0.6	0.4	0.18
BBK	Bushbuck	40	59	4.5	588	0.7	0.22	6.8	196	0.3	0.8	0.2	0.02
KG172	Kongoni	44	89	3.3	665	0.4	0.07	6.4	131	0.5	1.4	0.7	0.03
WB87	Wildebeest	46	80	3.2	508	0.6	0.07	6.8	154	0.3	0.7	0.5	0.02
WB88	Wildebeest	59	69	5.0	595	0.6	0.15	7.2	141	0.3	0.9	0.4	0.04
WB114	Wildebeest	57	67	4.9	722	0.8	0.12	9.2	160	0.2	1.0	0.5	0.07
Range of horn samples													
Min			21	2.8	437	0.3	0.07	5.2	131	0.2	0.5	0.2	0.02
Max			89	9.0	1110	1.2	0.22	9.2	215	0.5	1.4	0.8	0.27

Table 3.3: Concentrations of trace elements in the hair segments. The unit of the elemental concentrations is mg/kg. The diameter changes of the hair segments after abrasion are shown in Figure 2.2 and Table 2.1.

Sample	Note	Weight (mg)	Mg	Al	Ca	Ti	Mn	Cu	Zn	Se	Sr	Ba	Pb
Elephant hair													
EH-a	abraded	41	103	6	471	0.5	3.5	9.1	90	0.7	2.0	0.6	0.03
EH-b	unabraded	58	190	228	712	12.3	13.4	9.6	88	0.9	3.5	5.9	0.16
EH-c	abraded	52	189	11	969	0.9	14.4	5.6	111	0.7	4.3	2.0	0.04
EH-e	abraded	37	299	13	1416	0.7	40.2	9.5	88	1.1	7.4	4.2	0.04
EH-f	unabraded	38	463	779	1790	43.9	63.3	9.5	96	1.1	10.7	24.3	0.21
EH-g	abraded	36	315	28	1591	1.6	54.1	10.3	97	1.0	8.2	6.7	0.05
Giraffe hair													
GH-a	abraded	10	193	81	597	0.4	0.3	3.9	101	1.3	0.5	2.4	0.08
GH-b	unabraded	14	183	50	639	0.8	0.8	3.6	80	1.2	0.5	1.9	0.03
GH-c	abraded	8	162	66	561	0.6	0.3	3.5	80	1.0	0.5	2.1	0.08
GH-e	abraded	7	155	102	662	0.7	0.9	4.4	89	0.9	0.7	2.0	0.28
GH-f	unabraded	10	209	26	826	0.8	6.0	3.3	79	1.3	1.3	2.4	0.05
GH-g	abraded	7	175	99	615	0.6	0.8	3.3	97	0.9	0.6	2.2	0.11

3.6 Al and Fe in elephant hair surface layer

3.6.1 120 laser line analyses across the surface layer

Previous study in our laboratory (Fernandez et al., 2015) has found that the cuticle of elephant hair shows damage at a distance of about 12 cm from the proximal end. The distal part of the hair is damaged by natural abrasion and has obvious surface cracks or scratches. Therefore, only hair segments from 0 to 12.4 cm from the root were analyzed.

One hundred and twenty laser-ablation line analyses on 55 cross sections along the elephant hair were performed. The laser transect on each cross section was from the center outwards: from medulla to cuticle through the cortex, and two examples of line analyses at different longitudinal distance, 22.1 mm and 61.3 mm, are shown in Figure 3.3. The Al laser profiles had sharp peaks at the surface layer, indicating a thin layer enriched in Al, and no resolvable signal in the internal part, indicating no or negligible inward diffusion. Fe profiles were very similar to Al profiles with sharp surface peak and no diffusion pattern. The results also show high heterogeneity of Al and Fe distribution in the surface layer of the hair. Even on one single cross section, Al or Fe peaks from different laser transects had very different peak height and peak width from each other. However, the shapes of the peaks were similar to each other and the heights of peaks markedly increased from the proximal end to the distal end. For instance, the peak maximum intensity increased by a factor 30 and 15 for Fe and Al, respectively, from 22.1 mm to 69.3 mm (Figure 3.3).

The increasing intensity of sharp peaks at the surface layer suggests the accumulation of these elements in the surface layer. Because the laser beam diameter is wider than the Al-rich layer, the maximum intensity of the peak on a laser profile (peak height) is controlled by both concentration and spatial distribution of Al in the surface layer. The peak height is therefore only a qualitative estimation of the Al concentration in the surface layer, rather than a quantitatively measurement. Moreover, due to the lack of an internal standard correction, the differences in height between peaks can represent differences either in concentration or in the thickness of the Al-rich layer. The peak width of Al and Fe is only controlled by the thickness of the surface layer. Therefore, peak width can be used as an indicator of the physical dimension of the surface layer, where Al and Fe reside. The peak width data are reported in Table 3.4. The cross sections at 12.3 mm and 13.9 mm from root were analyzed, but Al and Fe intensity were under their detection limits.

The Fe and Al peaks were sharp and independent peaks, the width of which can be measured. Figure 3.4 compares the widths of Fe and Al peaks. The majority of these peaks had widths between 20 um and 60 um. A few of them were wider than 60 um. Two laser

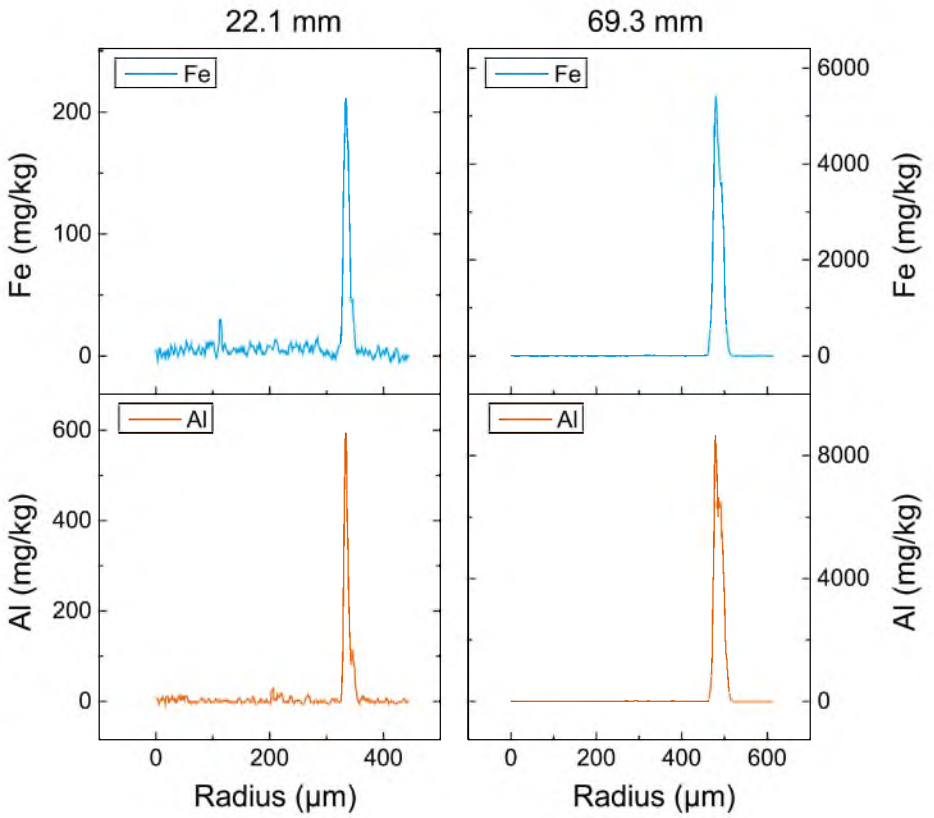

Figure 3.3: In-situ concentration of Al and Fe by laser ablation on two cross sections of the elephant hair at the distance of 22.1 mm and 61.3 mm, respectively, from the proximal end. Laser tracks move from the center of the cross section outwards.

moving speeds were used in this experiment: 3 μm/s and 4 μm/s (Table 3.4). Despite the speed differences among the measurements, the Al peak and the Fe peak of each single line analysis had the same shape (Figure 3.3) and similar width (Figure 3.4). The 1:1 correlation between the Fe-peak widths and the Al-peak widths indicates that these two elements are contained in the same region, defined as Al, Fe-rich surface layer, and behave similarly.

Al peak width generally increased (points in shaded area in Figure 3.5) from the proximal end to the distal end in the elephant hair. As water insoluble elements, Al and Fe would be unlikely to diffuse into the internal structure of hair. In turn, the increasing trend of the peak width suggests a continuous deposition of mineral particles containing both Al and Fe in the surface layer. Several transects containing Al peaks much wider than the general trend—shaded area in Figure 3.5—were observed. They may indicate places where the cuticle was broken or incomplete with cracks penetrating the cortex where insoluble particles can be confined.

Table 3.4: Laser line analyses on the elephant hair cross sections.

Segment ID	Section ID	Longitudinal distance (mm)	Laser line ID	Laser velocity (µm/s)	Peak width (µm)	
					Al	Fe
EH-3	EHC-111	12.3	111L	3	-	-
			111R	3	-	-
EH-4	EHC-112	13.9	112U	3	-	-
			112D	3	-	-
EH-5	lost					
EH-6	EHC-113	17.9	113U	3	45.0	45.0
			113D	3	31.8	31.8
EH-7	EHC-114	20.0	114U	3	28.5	27.5
			114D	3	22.0	19.8
EH-8	EHC-115	22.1	115L	3	23.1	22.0
			115R	3	37.3	34.0
EH-9	EHC-121	23.8	121L	3	23.1	23.1
			121R	3	37.3	38.4
EH-10	EHC-122	25.4	122L	3	23.1	25.3
			122R	3	27.5	27.5
EH-11	EHC-123	27.4	123L	3	22.0	24.2
			123R	3	45.0	48.3
EH-12	EHC-124	29.4	124U	3	17.6	19.8
			124D	3	18.7	22.0
			124L	3	37.3	35.1
			124R	3	24.2	41.7
EH-13	EHC-125	31.3	125D	3	26.4	24.2
			125U	3	35.1	37.3
			125R	3	31.8	31.8
EH-14	EHC-126	33.2	126U	3	29.6	29.6
			126D	3	26.4	26.4
			126L	3	35.1	32.9
			126R	3	32.9	28.5
EH-15	EHC-127	35.0	127L	3	31.8	32.9
			127R	3	31.8	30.7
EH-16	EHC-131	36.9	131U	3	20.9	26.4
			131D	3	-	-
			131L	3	28.5	30.7
EH-17	EHC-132	38.8	132L	3	25.3	28.5
			132R	3	47.2	46.1
EH-18	EHC-133	40.6	133U	3	29.6	30.7
			133D	3	25.3	27.5
EH-19	EHC-134	42.5	134U	3	34.0	35.1
			134R	3	31.8	32.9
			134L	3	30.7	35.1
EH-20	EHC-135	44.4	135U	3	24.2	27.5

Table 3.4 Continued

Segment ID	Section ID	Longitudinal distance (mm)	Laser line ID	Laser velocity (µm/s)	Peak width (µm)	
					Al	Fe
			135D	3	28.5	31.8
EH-21	EHC-136	46.1	136L	3	27.5	30.7
			136R	3	28.5	30.7
EH-22	EHC-137	47.9	137D	3	25.3	29.6
			137U	3	23.1	28.5
EH-23	EHC-141	50.1	141U	4	22.0	27.8
			141D	4	32.2	33.7
EH-24	EHC-142	52.0	142L	4	32.2	32.2
			142R	4	33.7	43.9
EH-25	EHC-143	53.7	143L	4	33.7	32.2
			143R	4	29.3	36.6
EH-26	EHC-144	55.5	144L	4	38.1	41.0
			144R	4	33.7	38.1
EH-27	EHC-145	57.5	145U	4	38.1	41.0
			145D	4	35.1	32.2
EH-28	EHC-146	59.4	146U	4	48.3	52.7
			146D	4	36.6	35.1
EH-29	EHC-147	61.3	147U	4	51.2	51.2
			147D	4	35.1	35.1
EH-30	EHC-151	63.4	151U	4	29.3	32.2
			151D	4	27.8	27.8
EH-31	lost					
EH-32	EHC-152	72.7	152U	4	39.5	42.5
			152D	4	29.3	30.7
			152L	4	29.3	27.8
			152R	4	42.5	41.0
EH-33	EHC-153	74.5	153U	4	26.4	29.3
			153D	4	30.7	32.2
EH-34	EHC-154	76.3	154L	4	39.5	36.6
			154R	4	63.0	61.5
EH-35	EHC-155	78.2	155U	4	36.6	38.1
			155D	4	35.1	32.2
EH-36	EHC-211	80.3	211R	3	50.5	50.5
			211D	4	36.6	33.7
EH-37	EHC-212	82.3	212D	4	27.8	33.7
			212U	4	38.1	35.1
EH-38	EHC-213	84.3	213U	4	45.4	54.2
			213D	4	27.8	32.2
EH-39	EHC-214	86.1	214D	4	30.7	30.7
			214U	4	29.3	30.7
EH-40	EHC-215	87.9	215U	4	33.7	38.1

Table 3.4 Continued

Segment ID	Section ID	Longitudinal distance (mm)	Laser line ID	Laser velocity (µm/s)	Peak width (µm)	
					Al	Fe
			215D	4	42.5	43.9
EH-41	EHC-221	89.8	221U	4	38.1	42.5
			221D	4	39.5	38.1
EH-42	EHC-222	91.7	222L	4	24.9	26.4
			222R	4	41.0	43.9
EH-43	EHC-223	93.7	223U	4	30.7	30.7
			223L	4	32.2	36.6
EH-44	EHC-224	95.6	224D	4	36.6	36.6
			224U	4	26.4	23.4
EH-45	EHC-225	97.6	225U	4	29.3	30.7
			225D	4	33.7	35.1
EH-46	EHC-226	99.4	226U	4	46.8	43.9
			226L	4	68.8	71.7
			226R	4	38.1	39.5
EH-47	EHC-227	101.3	227L	4	48.3	42.5
			227R	4	39.5	42.5
EH-48	EHC-231	103.5	231R	4	46.8	43.9
			231D	4	54.2	52.7
EH-49	EHC-232	105.3	232L	4	33.7	33.7
			232R	4	42.5	41.0
EH-50	EHC-233	106.9	233D	4	42.5	41.0
			233U	4	30.7	30.7
EH-51	EHC-234	108.6	234L	4	42.5	42.5
			234R	4	48.3	46.8
EH-52	EHC-235	110.4	235L	4	29.3	27.8
			235R	4	98.1	96.6
EH-53	EHC-236	112.3	236L	4	29.3	33.7
			236R	4	79.1	82.0
EH-54	EHC-237	114.2	237L	4	36.6	35.1
			237R	4	41.0	41.0
EH-55	EHC-238	116.2	238L	4	45.4	41.0
			238R	4	48.3	48.3
EH-56	EHC-241	118.0	241L	4	38.1	39.5
			241R	4	36.6	36.6
EH-57	EHC-242	120.0	242U	4	38.1	39.5
			242D	4	26.4	38.1
EH-58	EHC-243	122.0	243L	4	26.4	30.7
			243R	4	30.7	29.3
EH-59	EHC-244	124.0	244U	4	79.1	79.1
			244D	4	38.1	41.0

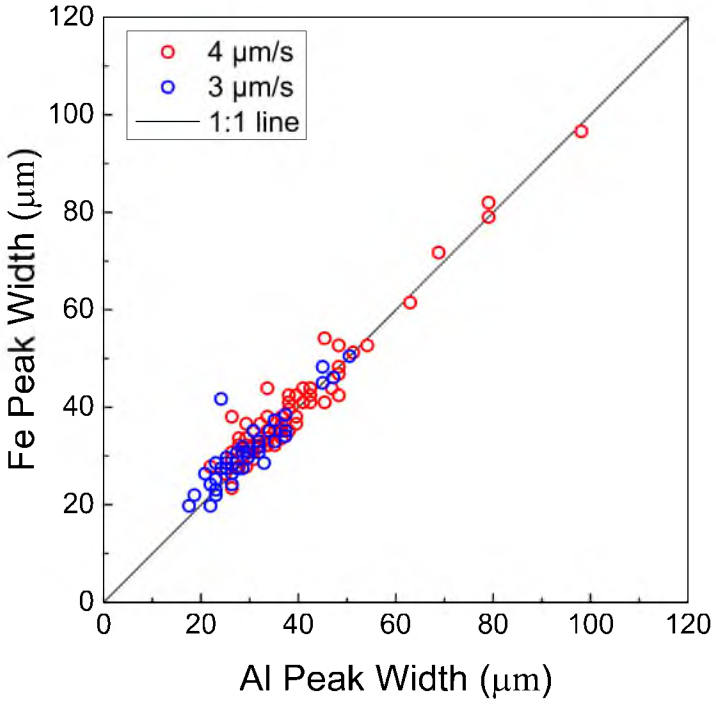

Figure 3.4: The comparison between Fe-peak widths and Al-peak widths of laser line-analyses on the cross sections of the elephant hair. Each point represents one single line-analysis. Red open circles and blue open circles represent the analyses with different laser moving speeds of 4 µm/s and 3 µm/s, respectively.

3.6.2 Surface layer on one cross section

One single cross section at the longitudinal distance of 76.3 mm from the proximal end was chosen to be analyzed with a small-size laser beam (7.2 µm diameter) for higher resolution (Figure 2.5). The Al peak widths and peak areas of all 26 transects on this cross section are reported in Table 3.5. The layer width was calculated by subtracting laser beam diameter from the peak width. The peak area was defined as the area under the laser profile across the surface layer. One example of line b is shown in Figure 3.6. The range of peak widths was from 10.8 to 20.2 µm.

The peak width and the peak area showed no trend or correlation (Figure 3.6), indicating a heterogeneous distribution of Al in the surface layer. Al profiles of all line analyses, except line a and line x, had sharp peaks at the surface layer. The absence of an Al peak on lines a and x indicates that the surface layer was not continuous and the gap on the surface layer was wider than 7.2 µm. All other lines had peaks wider than 7.2 µm, indicating that the surface layers crossed were probably complete. The calculated surface layer width was from 3.6 µm to 13.0 µm.

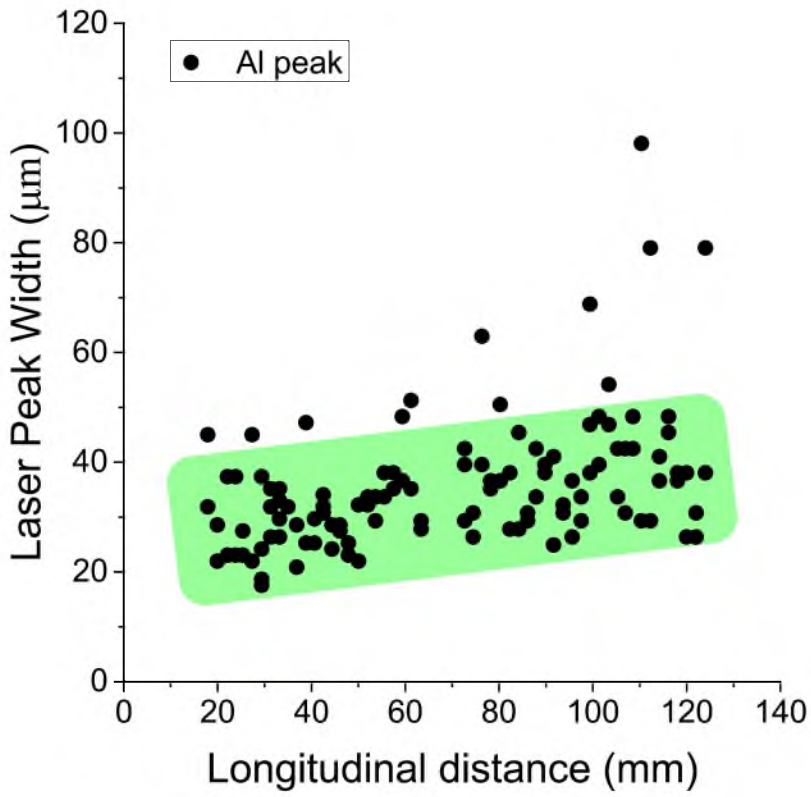

Figure 3.5: Compilation of Al peak width vs. distance from proximal end of all laser analyses on the cross section of the elephant hair. The laser beam is a circular beam with 31.4 µm diameter.

3.7 Sr in horse tail hair segments

The Sr concentration and Sr isotopic composition of ten horse tail hair segments were measured (Table 3.6). HB-1 was the hair root including the part under the skin and should represent a partly endogenous signal. HB-10 was the second to last segment on the distal end. HB-9 and HB-10 segments were longer than other segments closer to the proximal end to compensate for the abrasive loss of mass. The segment HB-10 had the lowest density, but the highest Sr concentration of all the segments measured for Sr.

The Sr concentration in the segments increased by a factor of 10 from 2.7 mg/kg to 25.8 mg/kg with increasing longitudinal distance. The segment HB-9 was below the general trend while the segment HB-3 was above the general trend (Figure 3.7). The recovery of Sr in column separation for all segments was larger than 50%. The incomplete recovery, considering the high partition coefficient of the resin, was probably due to the leakage during the loading step because of the extremely high HNO_3 concentration of the sample loading solution.

The $^{87}Sr/^{86}Sr$ ratio also increased from the proximal end to the distal end with a range of

Table 3.5: Laser analyses on the cross section EH154 (76.3 mm from proximal end); 26 laser transects showing Al concentration with estimates of the width of surface contamination.

Line ID	Peak width (µm)	Skin width (µm)	Area of peak (mg/kg × µm)
a	-	-	-
b	20.2	13.0	5.3×10^5
c	17.1	9.9	2.4×10^5
d	17.1	9.9	2.9×10^5
e	11.6	4.4	9.1×10^4
f	10.8	3.6	9.0×10^4
g	11.4	4.2	1.5×10^5
h	15.4	8.2	1.2×10^5
i	12.3	5.1	1.1×10^5
j	10.8	3.6	3.6×10^4
k	14.1	6.9	6.4×10^4
l	17.1	9.9	1.2×10^5
m	11.0	3.8	3.5×10^4
n	13.3	6.1	6.3×10^4
o	15.0	7.8	1.2×10^5
p	12.7	5.5	2.8×10^5
q	12.9	5.7	1.2×10^5
r	14.8	7.6	3.2×10^5
s	15.2	8.0	3.7×10^5
t	16.2	9.0	9.0×10^4
u	11.6	4.4	2.2×10^5
v	11.9	4.7	1.0×10^5
w	17.1	9.9	1.0×10^5
x	-	-	-
y	12.9	5.7	8.1×10^4
z	15.0	7.8	1.0×10^5

0.7087 to 0.7109 (Figure 3.7). The unidirectional increasing trend of both Sr concentration and $^{87}Sr/^{86}Sr$ ratio indicates a continuous addition of Sr from the environment. This 66-cm-long hair covered about 20 months of hair growth time, and there was no obvious seasonal variation in either Sr concentration or Sr isotopic composition during this period.

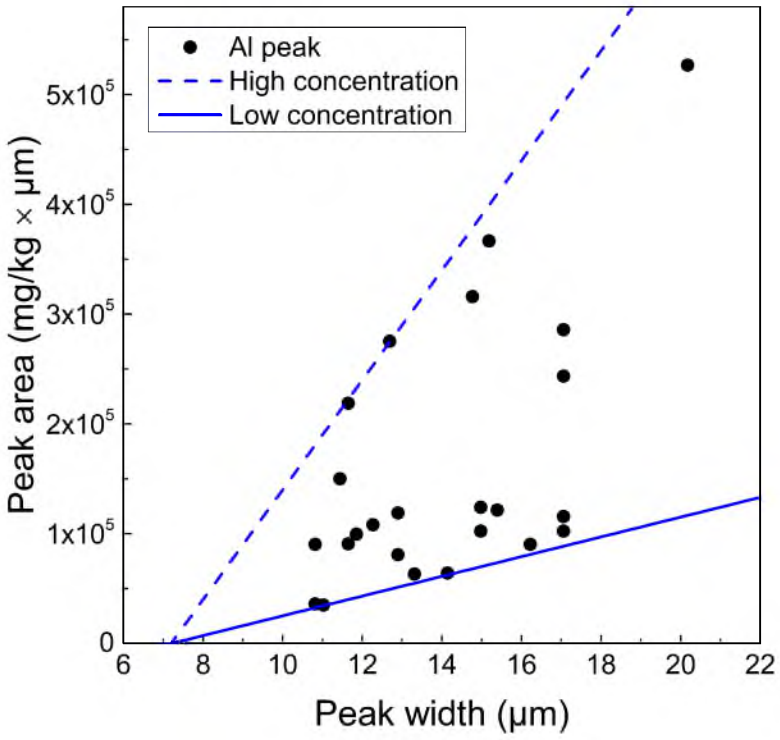

Figure 3.6: The area vs. the width of Al peak on the cross section of the elephant hair at a distance of 76.3 mm from the proximal end. The two lines are the result of a laser passing continuous and homogenous layers with different thickness at high and low Al concentrations. Graphic representation of these this concept can be seen in Figure 4.3 and Figure 4.4.

Table 3.6: Sr concentration and isotopic composition of the horse tail hair segments.

Segment ID	Length (mm)	Weight (mg)	Density (mg/mm)	Sr content (mg/kg)	$^{87}Sr/^{86}Sr$
HB-1	32.1	1.45	0.045	2.7	0.7087 ± 0.0002
	30.2 *				
HB-2	30.9	1.28	0.042	2.5	0.7096 ± 0.0002
	30.7 *				
HB-3	30.3	1.33	0.044	4.2	0.7097 ± 0.0002
	30.8 *				
HB-4	29.9	1.35	0.045	3.0	0.7096 ± 0.0002
	30.7 *				
HB-5	30.5	1.38	0.045	3.4	0.7100 ± 0.0002
	31.6 *				
HB-6	32.7	1.41	0.043	5.8	0.7106 ± 0.0002
	32.7 *				
HB-7	30.7	1.37	0.045	8.5	0.7104 ± 0.0002
	30.1 *				
HB-8	31.5	1.36	0.043	14.9	0.7106 ± 0.0002
	30.4 *				
HB-9	40.8	1.67	0.041	14.1	0.7107 ± 0.0002
	39 *				
HB-10	39.7	1.45	0.037	25.8	0.7108 ± 0.0002
	40.8 *				

From HB-1 to HB-10 is from the proximal end to the distal end of hair.
* Those segments were not analyzed. Only the ten marked segments were analyzed.

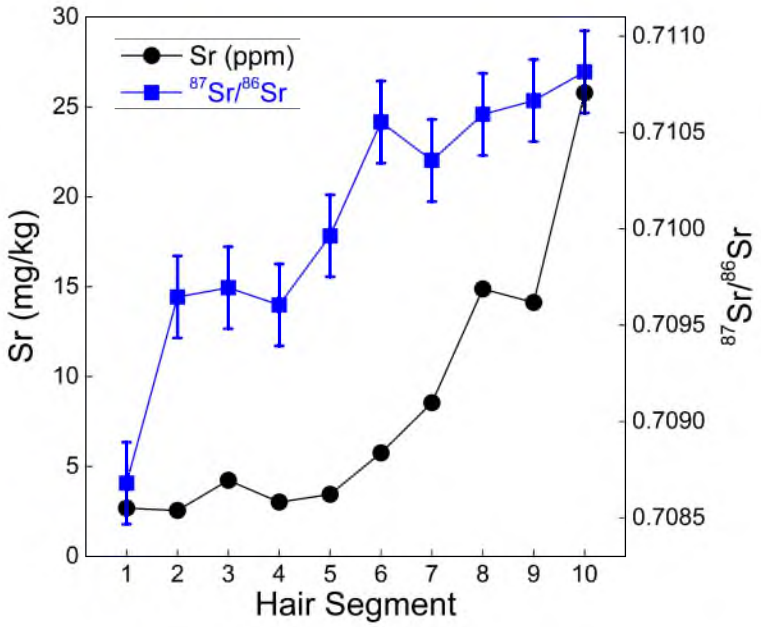

Figure 3.7: Sr concentration and Sr isotopic composition in the horse tail hair segments.

CHAPTER 4

DISCUSSION

4.1 Contamination and diffusion in hair

Renshaw, Pounds, and Pearson (1972) found a sequential increase of the Pb concentration in human hair segments from root to tip, which suggested environmental contamination of Pb in the hair shaft. Later study on the spatial distribution of trace elements in human hair found exogenous trace metals accumulated in the surface layer, resulting in longitudinal concentration increases of trace metals on the outer surface (Cookson & Pilling, 1975; Kempson & Skinner, 2005). Besides the surface contamination, the exogenous signal of trace metal within the hair shaft has also been identified. Mérigoux et al. (2003) found that a significant portion of internal Ca on human hair cross section, as calcium soap, was easily removable by hydrochloric acid, which likely had both endogenous and exogenous origin.

The results of this study suggest that the exogenous portion of several trace elements in the internal structure of hair was transported from surface contamination inward by diffusion. The differences of the intensity and the width of Al peaks between the two sides of elephant hair cross section (Figure 3.1 and Table 3.4) represent heterogeneous accumulation of this insoluble element from environmental contamination. Soluble elements, like Mg, have a diffusive pattern (Figure 3.1), represented by an enriched surface layer with decreasing intensity inward, indicating an accumulation in surface layer followed by a diffusion into the internal part of the hair shaft. Previous study in our laboratory (Fernandez et al., 2015) has found Sr, also a soluble element in water, can diffuse into the internal structure of elephant hair and has a similar diffusion pattern as Mg.

Elephants drink and bath daily when water is available. Following drinking, elephants bathe in water and even submerge completely in deep water when a large water pool is available. If the amount of water is limited, an elephant can use its trunk as a hose to wet itself (Estes, 1991). Giraffes can fill much of their need for water from green leaves and do not often get their bodies into water. In this study, I consider the animals spending extended time in water, like elephants, as "wet" animals, and the animals who do not spend

much time in water, like giraffes, as "dry" animals.

The cuticle of hair works as a protective layer to protect the hair shaft from mechanical and thermal damage. It is made up of large flat cells (called scales) imbricated on the surface of hair (Dawber & Comaish, 1970), which allows moisture to move in and out through the interspace between the scales. While the cuticle is in an aqueous environment, the scales open up to absorb dissolved ions and to adsorb insoluble particles in water, resulting in a surface layer that is enriched in trace elements. The longer the hair stays in water, the more trace element contamination will accumulate in the cuticular region, while some elements can then diffuse into the internal part of the hair. "Wet" animals should therefore have higher concentrations of trace elements in hair, in both the surface layer and the internal part, than "dry" animals. Our results support this hypothesis as we see the hair from the elephant, a "wet" animal, have orders of magnitude higher concentrations of trace elements than the hair from the giraffe, a "dry" animal.

Although the accumulation of trace elements in the surface layer of hair occurs in the surface water like rivers or lakes, the diffusion of soluble elements between the surface layer and the internal part of hair may occur during the moisture exchange of the hair with the rainwater. The endogenous portion of soluble element on the surface layer may also be leached out during the contact with the rainwater.

4.2 Endogenous levels of trace elements in clean keratin

Compared to the chemical washing methods, physically removing the hair outer surface is a more effective method to remove the contamination without leaching of the internal signal. As more than 1 mm of the most outer part of the horn has been removed, the trace elements in the interior of horn samples should be mostly endogenous (Figure 3.2).

The ranges of the concentrations of measured trace elements in the horn interiors, except for Pb, are much smaller than the variations in the measured hair interiors (Table 3.2 and Table 3.3) and in the reference values from Goullé et al. (2005) and Rodushkin and Axelsson (2000), suggesting that the horn interior is much less contaminated than hair samples. Therefore, with minimized environmental contamination, the ranges of trace element concentrations of horn interiors are used as the reference endogenous levels of trace elements in keratin.

Pb in horn interiors had a much larger range than other elements in horn interiors, which represents location difference: the Antelope Island bison (BH samples) had a higher concentration range from 0.06 mg/kg to 0.27 mg/kg while those African animals had a lower concentration range from 0.02 mg/kg to 0.07 mg/kg (Table 3.2). Such difference may be

due to the urban contamination of the Antelope Island bison from the nearby metropolitan area, the Salt Lake valley.

4.3 Different groups of trace elements in hair

Besides in-situ laser analysis, mechanical removal of the hair surface provides another way to study the spatial distribution of elements in hair (Figure 4.1). This method allows direct comparison of trace elements among different regions of the hair shaft with accuracy which laser analysis lacks. The difference between the internal signal (abraded segments) and the bulk signal (unabraded segments) reflects the abundance of trace elements in surface layer, where a major portion of contaminants reside. Zn, Cu and Se in both elephant and giraffe hair show little difference between abraded and unabraded segments (Figure 4.1), indicating a predominantly endogenous source of these elements. Most elements in elephant hair show longitudinal increases of concentration for two unabraded segments [$c_i(f) > c_i(b)$, where $c_i(x)$ represents the concentration of element i in segment x] (Figure 2.1 and Figure 4.1) and longitudinal concentration increase of internal intensity for four abraded segments [$c_i(g) > c_i(e) > c_i(c) > c_i(a)$]. The longitudinal increase of the concentration of these elements in unabraded segments suggests an accumulation of external contamination on the surface of elephant hair, while the longitudinal concentration increase in abraded segments suggests a continuous add-in of exogenous signal diffused from the surface into the interior of elephant hair for these elements.

Environmental contamination can accumulate in the surface layer of horns and hairs and then migrate into the internal keratin structure, which changes the bulk composition and may change the internal concentration of trace elements, respectively (Kempson & Lombi, 2011). Animal horns' larger diameter can minimize the exogenous signal of trace elements in the internal part migrated from the surface inward. Mammalian horns are made of the same type of keratin as mammalian hairs (Block, 1951). Trace element concentration ranges measured in horn interiors can then be used as a reference of endogenous level of these elements in keratin.

While all contaminants generally accumulate in the surface layer, likely the cuticle, they may or may not be transported into the internal structure of hair. Therefore, I divided the trace elements into four groups based on their similarity of spatial distribution and diffusive behavior in the elephant and the giraffe hairs (Table 4.1). This classification provides an understanding of those selected trace elements in hair and can help the future study of human hair.

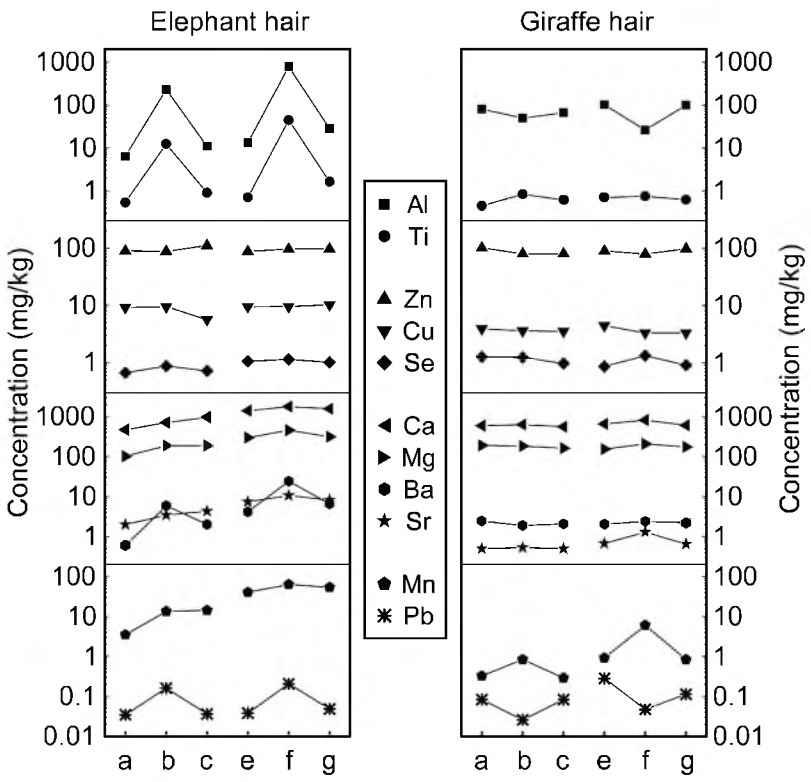

Figure 4.1: Comparison of abraded and unabraded hair sections for the elephant hair and the giraffe hair. Segments a, c, e, and g are abraded; Segments b and f are unabraded.

4.3.1 Insoluble elements: Al and Ti

Due to the lesser importance of Al for human health and environment, there are not many keratin studies reporting the concentration of this element. In hair studies that report Al, bulk analyses gave wide ranges of Al abundance from 8.2 to 74.1 mg/kg (Bermejo-Barrera, Moreda-Piñeiro, Moreda-Piñeiro, & Bermejo-Barrera, 1998) and from 2.7 to 25.6 mg/kg (Rodushkin & Axelsson, 2000). One reference value of Al concentration in human hair reported by Goullé et al. (2005) also had a wide range from 0.26 mg/kg to 5.30 mg/kg. In-situ laser ablation analyses of human fingernails showed an Al-enriched surface layer with the mean concentration at 41 mg/kg compared to a much lower mean interior concentration of 0.62 mg/kg (Rodushkin & Axelsson, 2003). Another in-situ analysis with estimated intensity measured by time-of-flight secondary ion mass spectrometry showed that the internal Al intensity in human hair above the scalp was very low while the Al intensity in the surface layer increased longitudinally (Kempson & Skinner, 2005). The findings in these studies are consistent with the extremely enriched Al surface layer (Figure 3.1) and longitudinal concentration increase of unabraded segments (Figure 4.1) in elephant hair found in this study. Those findings suggest that Al in hair is dominated by external

Table 4.1: Classification of eleven trace elements in hair.

Group		Elements	Surface enrichment	Diffusivity	Longitudinal increase
i	Insoluble	Al, Ti	Extremely enriched	Very low	Yes
ii	Physiological	Cu, Zn, Se	Negligible or no enrichment	Low	No
iii	Alkaline earth	Mg, Ca, Sr, Ba	Moderately enriched	High	Yes
iv	Special	Mn, Pb	Moderately enriched	High	

contamination accumulated in surface layer, causing the large variation of Al concentration in bulk analysis. The Al-enriched surface layer could be due to the capture of colloidal or mineral particles when the cuticle scales were open when exposed to water. There is also a small degree of longitudinal increase of Al concentration in abraded segments in elephant hair (from 6 to 11 to 13 to 28 mg/kg), indicating diffusion of exogenous Al from the surface into hair interiors. However, considering laser profiles show no sign of diffusion (Figure 3.1) and the surface layer has three orders of magnitude higher Al intensity than the internal part (Figure 3.1), the diffusivity of Al in hair must be extremely low.

In giraffe hair, the intensity of the Al peaks on the surface layer is comparable to the small peaks near the center (Figure 3.1) and the Al concentration in an unabraded segment is lower than in the abraded segments nearby (Figure 4.1). The difference between the Al laser profiles of giraffe and elephant hairs suggests that the giraffe hair has negligible amount of surface contamination for Al. The internal Al concentration in giraffe hair (66–99 mg/kg) is about ten times higher than that of horn interiors (2.8–9.0 mg/kg), indicating that giraffe hairs may have more internal Al incorporated by physiological processes than elephant hair and all the horns tested.

The difference in Al spatial distribution between elephant hair and giraffe hair indicates "dry" animals have lower environmental contamination in hair while "wet" animals can have a substantial amount, which can be one order of magnitude more than the endogenous portion in mass. Modern humans take showers regularly, so humans can be considered wet or semi-wet. I expect high environmental Al contamination from water in human hair, which is consistent with the wide range of Al found in previous studies (Bermejo-Barrera et al., 1998; Goullé et al., 2005; Rodushkin & Axelsson, 2000). The measurement of Al concentration in hair using bulk analysis varies due to the nonuniform surface enrichment of environmental signal and therefore can be unreliable.

Similar to Al, Ti has an extremely enriched surface layer intensity with a relatively low internal intensity in elephant hair (Figure 4.1) and a wide natural range in human hair from 0.94 to 16.1 mg/kg (Rodushkin & Axelsson, 2000), suggesting the major portion of such a high Ti content in hair is from contamination as Al does. The longitudinal increase of Ti in unabraded segments (43.9 mg/kg > 12.3 mg/kg) indicates an accumulation of contamination on the surface layer, similar to the surface longitudinal increases found in human hair (Kempson & Skinner, 2005). Ti also has more than one order of magnitude higher concentration in unabraded segments than in abraded segments in elephant hair (12.3 vs. 0.5 and 0.9 mg/kg; 43.9 vs. 0.7 and 1.6 mg/kg), indicating a low diffusivity.

The range of Ti concentrations in abraded giraffe hair segments (0.4–0.7 mg/kg) overlaps with the range of Ti in abraded elephant hair segments (0.5–1.6 mg/kg) and the horns' interiors tested (0.3–1.2 mg/kg) (Figure 4.2). This agreement within a relatively narrow concentration range indicates a similar Ti binding mechanism during keratin synthesis.

4.3.2 Physiological elements: Cu, Zn and Se

Cu, Zn and Se are the most studied trace elements in hair as essential elements. They have the smallest differences between abraded and unabraded segments of elephant hair (Figure 4.1) and narrowest variations of internal intensity among the horns tested (Figure 4.2). The laser profile of Zn shows an internal-dominated pattern. Studies show that bulk Zn concentrations in hair and nail are relatively constant (Martin, Kempson, Naftel, & Skinner, 2005; Rodushkin & Axelsson, 2000; Sukumar & Subramanian, 2007) and that Zn concentration in hair is not affected by washing procedures using (1) detergent (sodium lauryl sulfate), (2) hexane and ethanol, respectively, or (3) acetone, anhydrous diethyl

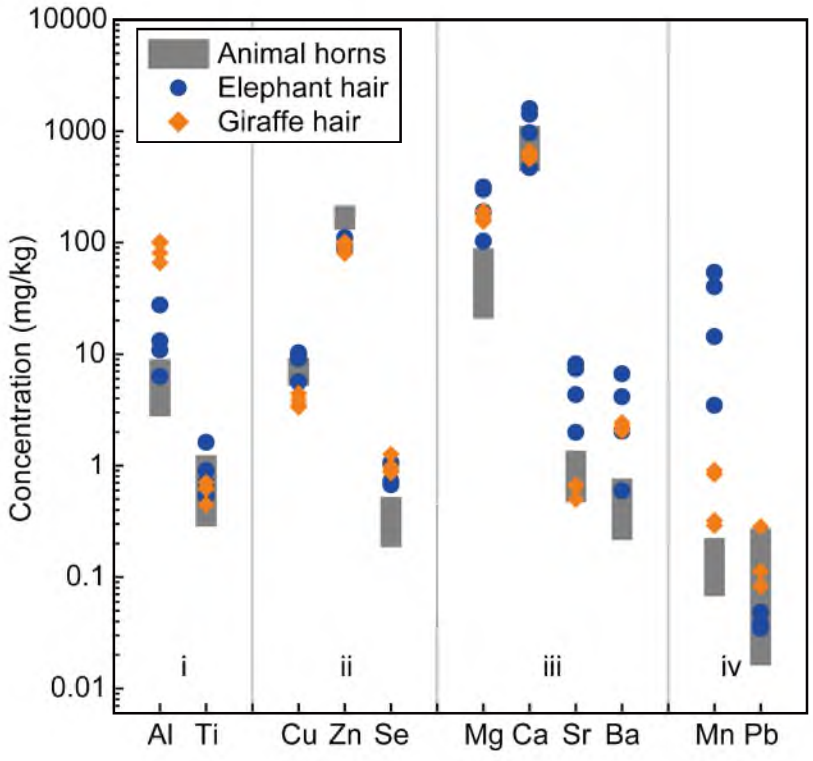

Figure 4.2: Trace element concentration of abraded hair sections compared to the range of trace element concentration of the horn interiors. The range of all thirteen horn interiors are shown as grey columns. Only abraded hair sections, a, c, e and g, are shown. Four groups of trace elements are shown in Table 4.1: (i) insoluble elements; (ii) physiological elements; (iii) alkaline earth elements; (iv) special elements.

ether and sodium lauryl sulfate solution, respectively (Assarian & Oberleas, 1977). Studies also show Cu and Zn are incorporated into the internal structure of human hair (Kempson, Skinner, & Kirkbridge, 2006) and have no longitudinal variation (Rendic, Holjevic, Valkovic, Zabel, & Phillips, 1976; Sera, Futatsugawa, & Murao, 2002). These observations support the conclusion that Cu, Zn and Se are endogenous trace elements related to physiological processes.

In this study, the similar pattern of Zn laser profiles in both elephant hair and giraffe hair cross sections suggests a predominantly endogenous source of Zn in hair. As one of the most abundant essential trace elements, the similarity of Zn concentrations in the elephant hair and the giraffe hair indicates similar physiological processes incorporating Zn into the hair structure during growth. It is reasonable to assume that Zn ingestion for elephants and giraffes living in different areas differs. So the similar anatomical variation of Zn in both hairs, shown in Figure 3.1, suggests the process of incorporating Zn into hair structure is independent of the Zn concentration in food and water. Zn and Se were found to have the same concentrations in the interiors of elephant and giraffe hair (80–111 mg/kg and 0.7–1.3 mg/g for Zn and Se, respectively) but different from the interiors of horns (131–215 mg/kg and 0.2–0.5 mg/g for Zn and Se, respectively) (Figure 4.2). In the case of Cu, however, elephant hair interiors and horn interiors have similar concentrations (5.2–10.3 mg/kg) that differ from giraffe hair interiors (3.3–3.9 mg/kg). These differences may indicate dissimilar physiological processes among the species represented in the samples analyzed.

The smallest variations of concentrations of these three elements in the horn samples analyzed do not only indicate an endogenous origin of these elements, but also imply that their concentrations do not reflect ingestion habits of the animals tested in this study. In humans, the variation of these elements in keratin could be caused by gender, age, color, race (Bertazzo et al., 1996; Taylor, 1986) or disease (Dastych, Cienciala, & Krbec, 2008; Sukumar & Subramanian, 2007) but not by the effect of sebum or dietary changes.

4.3.3 Alkaline earth elements: Mg, Ca, Sr, Ba

Although the surface layer signal of trace elements on the surface of hair is usually overwhelmed by the exogenous signal, the internal signal does not necessarily represent only an endogenous source due to the diffusion of contaminants from the surface to the internal structure of hair. Alkaline earth elements can significantly diffuse into the interior of hair and thus play an important role in the internal concentration of these elements.

Kempson and Skinner (2005) showed both Mg and Ca had enriched surface layer concentrations and a slight increase in medullar concentration, indicating a contamination on the

surface and a possibly enriched endogenous proportion in the medulla. Smart et al. (2009) claimed that the accumulation of Ca in the cuticle was related to the sulfur-rich regions in the cuticle, specifically the A-layer and exocuticle. For the internal Ca in hair, Mérigoux et al. (2003) demonstrated that two types of Ca existed: (1) free Ca^{2+}, easily removable by hydrochloric acid, carried by natural calcium soap into the cortex, the cuticle and the core of medulla; (2) protein-bound Ca^{2+}, which is not easily removable by hydrochloric acid, in the wall of medulla. While the protein-bound Ca^{2+} is probably incorporated into the hair structure by physiological processes, the free Ca^{2+} may have both endogenous and exogenous sources.

The enriched surface layer of Mg and the minor increases in medullary concentration as shown in the laser profiles (Figure 3.1) are consistent with the patterns found in Mg and Ca profiles from Kempson and Skinner (2005). My results also show longitudinal concentration increases of alkaline earth elements in both abraded [$c_i(g) > c_i(e) > c_i(c) > c_i(a)$] and unabraded segments [$c_i(f) > c_i(b)$] of elephant hair (Figure 4.1), suggesting that exogenous contaminants diffused from the surface into the internal structure of the hair.

The high physiological levels of Mg and Ca in horns (21–89 mg/kg and 437–1110 mg/kg, respectively) indicate considerable contribution of endogenous sources of these two elements (Figure 4.2). The highest level and smallest variation of internal Ca concentration indicates that the total Ca in the samples measured here was dominated by the endogenous Ca incorporated during keratin growth. Although there may be later exchange between internal and external Ca in hair carried by calcium soap (Mérigoux et al., 2003), the total Ca does not change much. As Sr and Ba have much lower physiological levels (0.5–1.4 mg/kg and 0.2–0.8 mg/kg, respectively), the exogenous signal can increase their bulk concentrations by a factor of up to 10 (6.7 vs. 0.6 mg/kg of Ba in elephant hair).

The differences between abraded and unabraded segments of Mg, Ca and Sr in elephant hair (factor of < 2) are much smaller than the differences of the insoluble elements, Al and Ti (factor of $\sim$40) (Figure 4.1, Table 3.3). Such small differences suggest a high diffusivity of these elements in hair, allowing exchanges between internal and external signals and a high solubility of these elements preventing the extreme accumulation found for Al and Ti. The difference between abraded and unabraded segments for Ba in elephant hair (factor of $\sim$5) is significantly larger than the difference for Mg, Ca and Sr (factor of < 2), likely because the lower solubility of Ba^{2+} in water allows more accumulation on the surface similar to the insoluble elements.

4.3.4 Special elements: Mn and Pb

Mn and Pb are grouped together, separately from other elements because they are the only two elements showing large longitudinal differences in abraded segments of the giraffe hair (Figure 4.1).

Mn in elephant hair shows a pattern similar to the alkaline earth elements with longitudinal concentration increases in both abraded [$c_{Mn}(g) > c_{Mn}(e) > c_{Mn}(c) > c_{Mn}(a)$] and unabraded [$c_{Mn}(f) > c_{Mn}(b)$] segments, indicating high diffusivity of Mn in the internal part of hair. Surprisingly, different from the other elements in giraffe hair, Mn shows obvious longitudinal concentration increases in unabraded segments [$c_{Mn}(f) > c_{Mn}(b)$], indicating an accumulation of external contamination. However, the reason that only Mn in giraffe hair contains environmental contaminants is still unknown. Considering giraffe hair has little water-related environmental contaminations, the variation of Mn may be a result of a different mechanism of adding exogenous signals. One possibility is that Mn has a different contamination source compared to the other elements, possibly an airborne Mn compound. Another possible reason is the difference between the basic pH condition for Mn to be optimally absorbed and the acidic pH condition needed for other trace elements (Sweileh, 2003). Mn can also diffuse into the internal structure of giraffe hair, causing the variation of Mn internal intensity observed in this case (Figure 4.1), which may occur while the hair is moistened by rainwater.

Although Martin et al. (2005) directly related their finding of enriched surface layer of Pb in human hair to external contamination, other studies have shown Pb in hair is correlated with Pb in blood for both human hair (Foo et al., 1993) and cow tail hair (Patra et al., 2007), indicating a significant portion of the Pb concentration found in hair also has an endogenous source.

Pb in elephant hair shows relatively small longitudinal increases in both unabraded segments (0.16 to 0.21 mg/kg) and abraded segments (0.03 to 0.04 to 0.04 to 0.05 mg/kg) (Figure 4.1), indicating less environmental contamination and lower diffusivity of Pb than most other trace elements. The internal Pb concentration in elephant hair is included within the range of horns and it is lower than giraffe hair. The difference between abraded and unabraded segments of elephant hair may reflect an enriched surface layer of Pb in hair caused not by continuous external contamination like Al but by physiological processes.

The unabraded giraffe hair segments have lower Pb concentrations than the nearby abraded segments [0.03 (segment b) < 0.08 (a) or 0.08 (c) mg/kg, 0.05 (f) < 0.28 (e) or 0.11 (g) mg/kg; Table 4.1], so the internal concentration of Pb is higher than the Pb concentra-

tion in the surface layer of the giraffe hair (Figure 4.1). Because endogenous elements have different binding sites (Langbein et al., 1999) and are distributed heterogeneously in hair, the center-concentrated spatial distribution of Pb in the giraffe hair indicates that Pb has a significant endogenous portion concentrated in medulla.

Although the spatial distribution of Pb in the elephant hair is different from the giraffe hair, Pb in both elephant and giraffe hair may be dominated by endogenous source. The location differences of Pb in horn samples (Table 3.2) may reflect the environmental difference of Pb ingested by the animals and incorporated into their horn interior.

4.4 Al and Fe in surface layer

As discussed before, insoluble elements like Al, Fe and Ti accumulate in the surface layer of hair and do not diffuse into the internal structure of hair. A detailed laser study along the hair provides a better understanding of the distribution of these elements in the surface layer and the correlation between each other. Sequential sampling and laser analyses can help understanding the changes in the surface layer. Four line analyses on two cross sections, EHC-111 (12.3 mm from proximal end) and EHC-112 (13.9 mm from proximal end), closest to the body have no detectable Al or Fe peaks (Table 3.4). The fact that I cannot detect Al and Fe under 12.3 mm while both Al and Fe intensity in the surface layer increases along the hair (Figure 3.3) confirms that both Al and Fe in elephant hair are derived from external contamination.

The peak width of insoluble Al and Fe can be used as an indicator for the thickness of the surface layer. If the layer were continuous, the thickness of the layer would be the peak width minus the laser beam diameter (Figure 4.3). If the layer were not continuous, the peak width would be controlled by both layer thickness and gap width (Figure 4.4). The laser study using a 7.2 μm beam includes two line analyses with no Al peak detected, indicating a discontinuity in the contaminated layer which has gaps wider than 7.2 μm.

If the layer on which the laser ablation moves across is continuous and homogeneous, the peak area of the laser profile should correlate linearly with the peak width or the surface layer width. The two lines in Figure 3.6 represent two continuous and homogeneous surface layers with low and high concentrations. However, the points in Figure 3.6 scatter in the plot and do not fall on either of the lines, indicating that the surface layer is not homogeneous. The slopes of the dashed line and the solid line, which bracket all points, differ by a factor of six, indicating the variation of the Al concentration in the surface layer can be as large as a factor of six on one cross section.

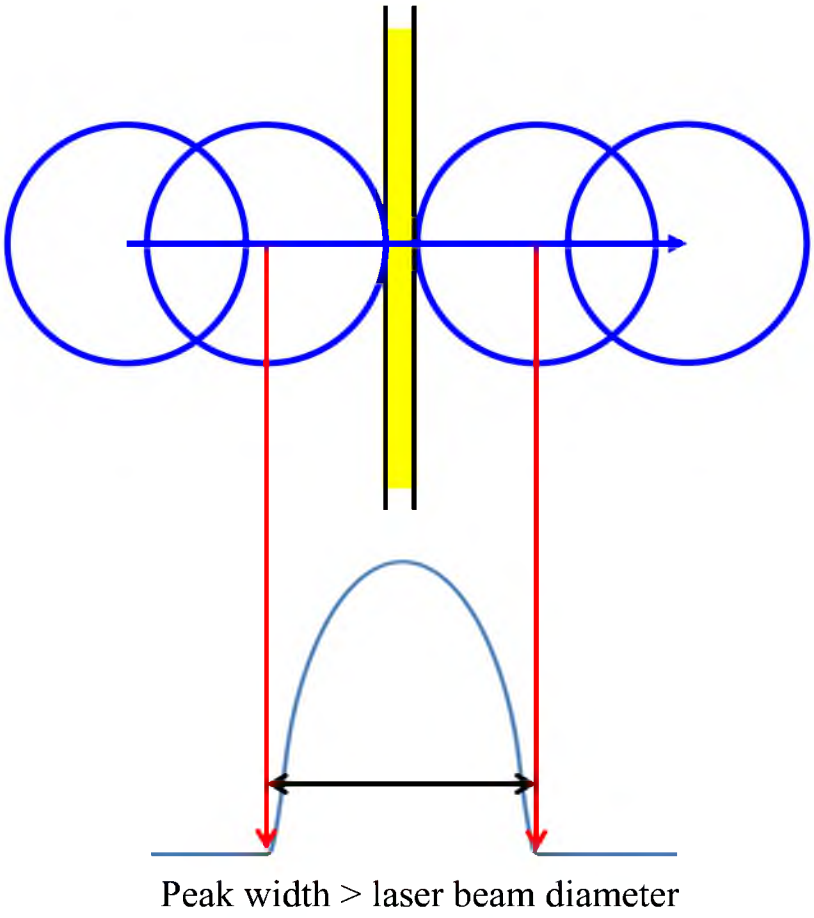

Figure 4.3: Peak width is wider than the laser beam diameter when the laser moves across the continuous part of a layer.

In the 120 laser-ablation line analyses on 55 elephant hair cross sections utilizing a 31.4 µm laser beam (section 3.6.1), the widths of both the Al peak and the Fe peak in many lines are narrower than 31.4 µm (Figure 3.4), suggesting the discontinuity of the surface layers on those cross sections. If the laser-ablation line passes through the gap in a surface layer wider than 31.4 µm, there will be no surface peak showing in the laser profile. There is only one line, line 131D on cross section EHC-131, of which neither an Al peak or a Fe peak was detected (Table 3.4) in the 120 laser-ablation line analyses. Therefore, the majority of the surface layer gaps are narrower than 31.4 µm. As discussed before, the cuticle is made up of imbricated scales where environmental contaminants can accumulate. The sizes of those scales are about a few µm to tens of µm depending upon the animal species. The discontinuity of the surface layer may represent the gap between two scales or an uncontaminated region. If the laser moves across a complete scale, as most 7.2 µm laser analyses did, the width of a Al peak is surely wider than the laser beam diameter (Figure

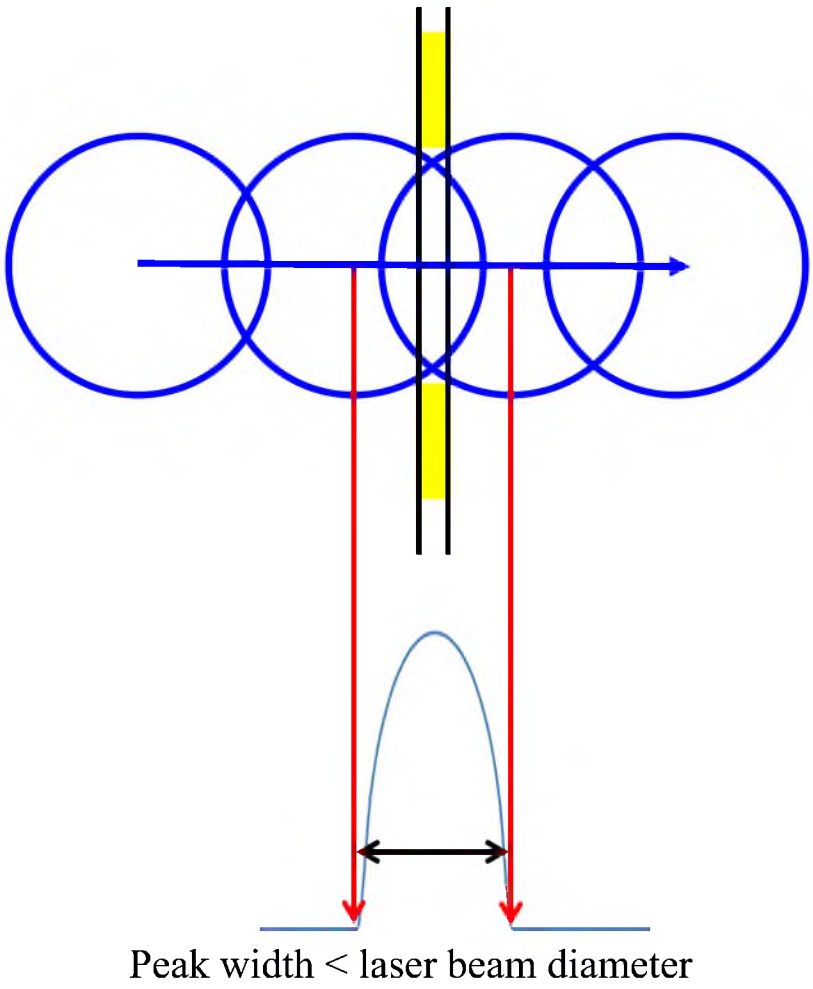

Figure 4.4: Peak width is narrower than the laser beam diameter when the laser moves across the discontinuous part of a layer.

4.3). If the laser moves across the gap, the width of a Al peak is expected to be narrower than the laser beam diameter (Figure 4.4), like those Al peaks whose widths are narrower than 31.4 µm laser beam diameter in Figure 3.5. As the surface layer of hair captures more and more insoluble contaminants, the layer will grow thicker. The laser analyses across those thickened layers would have wider Al peak width over time, like the trend of green background in Figure 3.5.

4.5 Study of external contamination of Sr

As an alkaline earth element found to be able to diffuse into the cortex (section 4.3.3), the Sr signal measured in hair can contain both endogenous source and exogenous sources. The horse tail hair is about 60 cm long, representing about 20 months of growing time. For all the segments measured from the proximal end to the distal end, there is no seasonal

variation observed in either Sr concentration or Sr isotopic composition (Figure 3.7). Even if the seasonal change may contribute to the isotopic variation of Sr, either it is overwritten by the large range of unidirectional shift shown in Figure 3.7 or it cannot be resolved due to the low resolution of time. The unidirectional changes of both concentration and isotopic composition suggest a continuous addition of Sr from the environment.

When $^{87}Sr/^{86}Sr$ vs. 1/Sr is plotted, a linear fit line can be assigned to those points (Figure 4.5). This straight line is an indication of the mixing of sources where a exogenous Sr source with a different $^{87}Sr/^{86}Sr$ ratio is added to the hair. The intercept where 1/Sr = 0 on the plot, of which the $^{87}Sr/^{86}Sr$ ratio is 0.7110, is the exogenous source. Chesson et al. (2012) did a study on the $^{87}Sr/^{86}Sr$ ratio of tap water in Salt Lake Valley, in which four of five samples had an average value of 0.7096 ± 0.0006 and the fifth sample had a value of 0.7124. Additional data for Salt Lake Valley tap water measured in our lab have an average value around 0.7110. The $^{87}Sr/^{86}Sr$ ratio of the intercept, 0.7110, in Figure 4.5 is within the range of Salt Lake Valley tap water. Considering the horses living in the stable are washed with tap water, the tap water is a possible source of exogenous Sr in the horse tail hair. Therefore, the addition of the exogenous signal in the horse hair not only changes its Sr isotopic composition but also increases its Sr concentration by a factor of ten. This observation highlights the problematic measurements of Sr isotopic composition and Sr concentration of hair samples: if total digestion of the hair with no cleaning procedure is performed, a major portion of the measured Sr will be related to the external contamination. Instead of the dietary signal, the Sr signal of the water used to wash the horse will be measured in the bulk analysis of hair.

The point HB-1 is off the fit line with an $^{87}Sr/^{86}Sr$ ratio different from the contiguous segments (Figure 3.7 and Figure 4.5). The gap between HB-1 point and the fit line could be due to its larger measurement uncertainty of concentration than other points with higher concentration. However, to move HB-1 point to the fit line, the measurement error of the concentration has to be larger than 20%, which is unlikely to be the case. Therefore, this gap probably represents a real difference of Sr composition between HB-1 and other segments. One possibility is that segment HB-1 received an extra exogenous addition of Sr, which was not added to other segments, causing HB-1 point moves through the path marked as the red arrow in Figure 4.5. However, considering segment HB-1 is the proximal end of the hair, it is hard to believe it contains extra contamination which other segments do not have.

Therefore, it is more likely that all hair segments, except HB-1, have lost a portion of

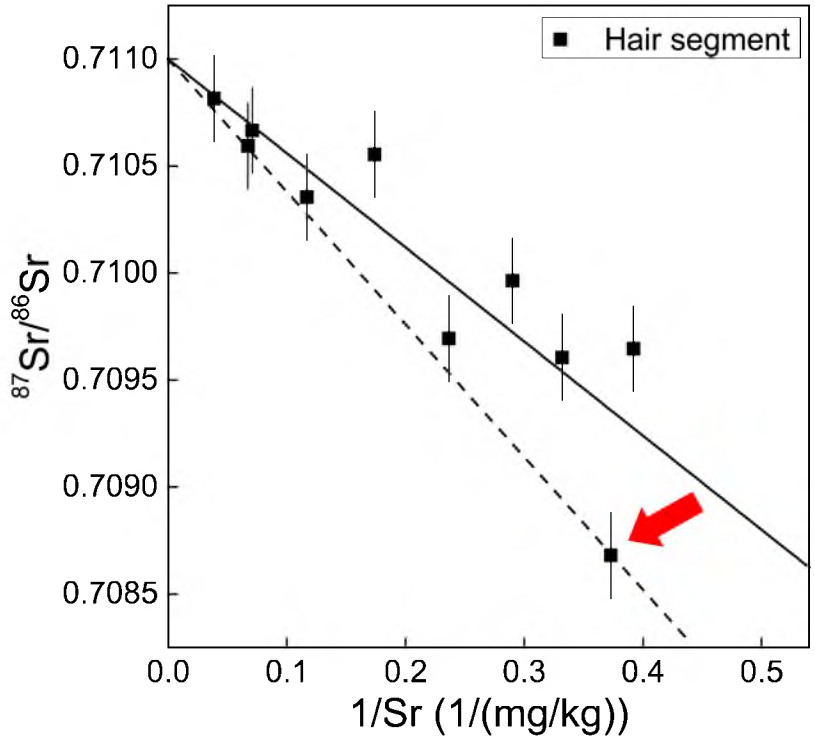

Figure 4.5: $^{87}Sr/^{86}Sr$ vs. 1/Sr of the horse tail hair segments. The solid line is fit line for all points: $y = -0.0044 \cdot x + 0.7110, R^2 = 0.78$. The dash line is a possible mixing line without the loss of original Sr in hair (see discussion in section 4.5). Red arrow represents a possible extra addition of exogenous Sr in HB-1 (see discussion in section 4.5).

original Sr, causing the shift of mixing line (from the dash line to the solid line in Figure 4.5). Such Sr loss process may occur after the hair grows outside of the skin where Sr can be leached out of the hair. This indicates that some part of the original endogenous Sr is removable and some part is fixed in hair structure, while the exogenous Sr accumulates on the surface of the hair and diffuses inwards. If an aggressive chemical cleaning method, like the 0.1 M HCl cleaning used by Tipple et al. (2013), is applied to remove more than 90% of Sr from hair, the $^{87}Sr/^{86}Sr$ value of residual Sr is likely to be the endogenous signal fixed in hair structure. However, the $^{87}Sr/^{86}Sr$ value of the exogenous source in hair is hard to obtain because the leachate may contain a fraction of the endogenous signal during leaching out exogenous signal. The result in this study suggests that segment cutting and a mixing model can be used to obtain both endogenous and exogenous signals in Sr isotopic analyses of hair, if the amount of sample is enough. If the dietary source does not change or its Sr isotopic variation is negligible relative to the difference between endogenous and exogenous sources, the $^{87}Sr/^{86}Sr$ value of the external contamination can be obtained from the intercept in mixing model and the $^{87}Sr/^{86}Sr$ value reflecting dietary information can be

obtained from the proximal segments.

4.6 Hair as an open system for trace elements

The concentration levels of trace elements within a single hair are not uniform, and change radially and longitudinally between and within the different components (cuticle, cortex and medulla). Elemental species, exposure time, behavior ("dry" vs. "wet") and hair condition (intact versus damaged cuticle) control the three-dimensional elemental distribution in the hair. Hair can be considered an open system undergoing a number of processes that determine the elemental level at each hair point.

Keratinization of animal horn incorporates physiological amounts of trace elements into the internal structure. Physiological levels of nonessential elements such as Al, Ti, Sr, Ba, etc. are found within a relatively narrow range (factor of 5) in horns of various species. Essential elements with relatively high internal concentration, like Zn, can be leached from hair.

Environmental contamination is embedded in the cuticular region of hair and horn. The amount of contamination increases as a function of time. Relatively soluble elements enriched in the cuticle diffuse from the contaminated cuticular region towards the cortical region. Relatively insoluble elements accumulate in the cuticular region with time.

CHAPTER 5

CONCLUSIONS

Environmental contamination of trace elements in keratinized structures (horn, hair, hoof, etc.) generally occurs in aqueous conditions where dissolved ions and particles can attach and accumulate within the surface layer over time. The migration of soluble elements between the surface contamination and the interior can also occur by means of aqueous diffusion, which alters the internal trace elemental abundance. Therefore, animals with different water-related habits ("wet" vs. "dry") have distinct bulk concentration of trace elements in hair due to different amounts of contamination. The hairs of "wet" animals—animals which spend an extended amount of time in water like elephants—contain substantial amounts of exogenous signals (e.g., 43.9 mg/kg Ti). The hairs of "dry" animals—animals which do not spend much time in water like giraffes—contain negligible amount of exogenous signals (e.g., 0.8 mg/kg Ti).

Identifying and separating the endogenous and exogenous portion of trace elements in hair is key to many applications of hair analysis, such as biological monitoring, study of pathological effects and forensic science. The environmental contamination of trace elements in keratin cannot be removed quantitatively by chemical cleaning methods. The concentrations of trace elements in horns, whose surface has been physically removed, have the least impact of environmental contamination because of its large size. Therefore, the surface-removed clean horn keratin can be used as reference material for the physiological levels of trace elements in keratin.

The concentrations of trace elements in the abraded hair segments provide information for the spatial distribution of trace elements in hair shafts when compared to the unabraded hair segments. Based on the comparison between horn and hair interiors and the comparison between abraded and unabraded hair segments, eleven trace elements can be divided into four groups of elements with distinct behaviors: (1) insoluble elements, including Al and Ti, which are extremely enriched in the surface layer and diffuse minimally into the internal structure of hair; (2) physiological elements, including Cu, Zn and Se, which are dominated

by the endogenous signal incorporated into the hair structure during hair growth; (3) alkaline earth elements, including Mg, Ca, Sr and Ba, which contain extensive amounts of endogenous signals but are significantly affected by the inward diffusion of exogenous signals; (4) special elements, like Mn possibly originated from airborne contamination, and Pb possibly reflecting ingestion. This classification offers a framework for the interpretation of trace elements in hair.

Two sources, endogenous and exogenous, with distinct Sr isotopic compositions in a horse tail hair were identified using the mixing model based on the result of sequential Sr isotopic analysis. The endogenous source, originated from food and drinking water, contributed ~2 mg/kg to the bulk Sr concentration in hair with an $^{87}Sr/^{86}Sr$ value of 0.7087. The exogenous source, probably from tap water used for washing, contributed more than 20 mg/kg to the bulk Sr concentration in hair with an $^{87}Sr/^{86}Sr$ value of 0.7110. Sequential analysis and an isotopic mixing model represent an effective method to study the trace elements with comparable contributions from both exogenous and endogenous sources.

REFERENCES

Assarian, G. S., & Oberleas, D. (1977). Effect of washing procedures on trace-element content of hair. *Clinical Chemistry*, *23*(9), 1771–2. Retrieved from http://www.clinchem.org/content/23/9/1771

Böhlke, J. K., de Laeter, J. R., De Bièvre, P., Hidaka, H., Peiser, H. S., Rosman, K. J. R., & Taylor, P. D. P. (2005). Isotopic compositions of the elements, 2001. *Journal of Physical and Chemical Reference Data*, *34*(1), 57–67. Retrieved from http://scitation.aip.org/content/aip/journal/jpcrd/34/1/10.1063/1.1836764 doi: 10.1063/1.1836764

Barbosa Jr, F., Tanus-Santos, J. E., Gerlach, R. F., & Parsons, P. J. (2006). A critical review of biomarkers used for monitoring human exposure to lead: advantages, limitations and future needs. *Ciência & Saúde Coletiva*, *11*(1), 229–241. doi: 10.1590/S1413-81232006000100032

Bermejo-Barrera, P., Moreda-Piñeiro, A., Moreda-Piñeiro, J., & Bermejo-Barrera, A. (1998). Determination of aluminium and manganese in human scalp hair by electrothermal atomic absorption spectrometry using slurry sampling. *Talanta*, *45*(6), 1147–1154. Retrieved from http://www.sciencedirect.com/science/article/pii/S0039914097002300 doi: 10.1016/S0039-9140(97)00230-0

Bertazzo, A., Costa, C., Biasiolo, M., Allegri, G., Cirrincione, G., & Presti, G. (1996). Determination of copper and zinc levels in human hair. *Biological Trace Element Research*, *52*(1), 37–53. doi: 10.1007/BF02784088

Block, R. J. (1951). Chemical classification of keratins. *Annals of the New York Academy of Sciences*, *53*(3), 608–612. doi: 10.1111/j.1749-6632.1951.tb31962.x

Brewer, P. A., Bird, G., & Macklin, M. G. (2016). Isotopic provenancing of pb in mitrovica, northern kosovo: Source identification of chronic pb enrichment in soils, house dust and scalp hair. *Applied Geochemistry*, *64*, 164–175. Retrieved from http://www.sciencedirect.com/science/article/pii/S0883292715300202 doi: 10.1016/j.apgeochem.2015.08.003

Cerling, T. E., & Harris, J. M. (1999). Carbon isotope fractionation between diet and bioapatite in ungulate mammals and implications for ecological and paleoecological studies. *Oecologia*, *120*(3), pp. 347-363. Retrieved from http://www.jstor.org/stable/4222397

Cerling, T. E., Wittemyer, G., Rasmussen, H. B., Vollrath, F., Cerling, C. E., Robinson, T. J., & Douglas-Hamilton, I. (2006). Stable isotopes in elephant hair document migration patterns and diet changes. *Proceedings of the National Academy of Sciences of the United States of America*, *103*(2), 371–373. doi: 10.1073/pnas.0509606102

Chesson, L. A., Tipple, B. J., Mackey, G. N., Hynek, S. A., Fernandez, D. P., & Ehleringer, J. R. (2012). Strontium isotopes in tap water from the coterminous usa. *Ecosphere*, *3*(7), art67. doi: 10.1890/ES12-00122.1

Chittleborough, G. (1980). A chemist's view of the analysis of human hair for trace elements. *Science of The Total Environment*, *14*(1), 53–75. Retrieved from `http://www.sciencedirect.com/science/article/pii/0048969780901266` doi: 10.1016/0048-9697(80)90126-6

Cookson, J. A., & Pilling, F. D. (1975). Trace element distributions across the diameter of human hair. *Physics in Medicine and Biology*, *20*(6), 1015. Retrieved from `http://stacks.iop.org/0031-9155/20/i=6/a=013`

Dastych, M., Cienciala, J., & Krbec, M. (2008). Changes of selenium, copper, and zinc content in hair and serum of patients with idiopathic scoliosis. *Journal of Orthopaedic Research*, *26*(9), 1279–1282. doi: 10.1002/jor.20629

Dawber, R., & Comaish, S. (1970). Scanning electron microscopy of normal and abnormal hair shafts. *Archives of Dermatology*, *101*(3), 316–322. doi: 10.1001/archderm.1970.04000030060009

Ehleringer, J. R., Bowen, G. J., Chesson, L. A., West, A. G., Podlesak, D. W., & Cerling, T. E. (2008). Hydrogen and oxygen isotope ratios in human hair are related to geography. *Proceedings of the National Academy of Sciences of the United States of America*, *105*(8), 2788–2793. doi: 10.1073/pnas.0712228105

Estes, R. D. (1991). *The behavior guide to african mammals: including hoofed mammals, carnivores, primates*. University of California Press. Retrieved from `http://www.ucpress.edu/book.php?isbn=9780520272972`

Faure, G., & Mensing, T. M. (2005). Mixing theory. In *Isotopes: Principles and applications* (pp. 347–362). John Wiley & Sons, Inc.

Fernandez, D. P., Cerling, T. E., Hynek, S. A., Brown, E. T., Anderson, C. R., & Topham, K. L. (2015). *Incorporation of trace elements in hair from the environment.* (Unpublished results)

Font, L., Nowell, G. M., Graham Pearson, D., Ottley, C. J., & Willis, S. G. (2007). Sr isotope analysis of bird feathers by tims: a tool to trace bird migration paths and breeding sites. *Journal of Analytical Atomic Spectrometry*, *22*(5), 513–522. doi: 10.1039/B616328A

Font, L., van der Peijl, G., van Wetten, I., Vroon, P., van der Wagt, B., & Davies, G. (2012). Strontium and lead isotope ratios in human hair: investigating a potential tool for determining recent human geographical movements. *Journal of Analytical Atomic Spectrometry*, *27*(5), 719–732. doi: 10.1039/c2ja10361c

Foo, S. C., Khoo, N. Y., Heng, A., Chua, L. H., Chia, S. E., Ong, C. N., ... Jeyaratnam, J. (1993). Metals in hair as biological indices for exposure. *International Archives of Occupational and Environmental Health*, *65*(1), S83-S86. doi: 10.1007/BF00381312

Gellein, K., Lierhagen, S., Brevik, P. S., Teigen, M., Kaur, P., Singh, T., ... Syversen, T. (2008). Trace element profiles in single strands of human hair determined by hr-icp-ms. *Biological Trace Element Research*, *123*(1-3), 250–260. doi: 10.1007/s12011-008-8104-0

Goullé, J.-P., Mahieu, L., Castermant, J., Neveu, N., Bonneau, L., Lainé, G., ... Lacroix, C. (2005). Metal and metalloid multi-elementary icp-ms validation in whole blood, plasma, urine and hair: Reference values. *Forensic Science International*, *153*(1), 39–44. Retrieved from http://www.sciencedirect.com/science/article/pii/S0379073805002082 doi: 10.1016/j.forsciint.2005.04.020

Hausman, L. A. (1920). Structural characteristics of the hair of mammals. *American Naturalist*, *54*(635), 496–523. Retrieved from http://www.jstor.org/stable/2456345 doi: 10.2307/2456345

Hobson, K. A., & Wassenaar, L. I. (1996). Linking breeding and wintering grounds of neotropical migrant songbirds using stable hydrogen isotopic analysis of feathers. *Oecologia*, *109*(1), 142–148. doi: 10.1007/s004420050068

Holloway, J. M., Ewing, S. A., & Maher, K. (2009). Combined ecological and geologic perspectives in ecosystem studies. *Chemical Geology*, *267*(12), 1–2. Retrieved from http://www.sciencedirect.com/science/article/pii/S0009254109002125 doi: 10.1016/j.chemgeo.2009.05.001

Iacumin, P., Davanzo, S., & Nikolaev, V. (2006). Spatial and temporal variations in the 13c / 12c and 15n / 14n ratios of mammoth hairs: Palaeodiet and palaeoclimatic implications. *Chemical Geology*, *231*(12), 16–25. Retrieved from http://www.sciencedirect.com/science/article/pii/S0009254105005437 doi: 10.1016/j.chemgeo.2005.12.007

Kempson, I. M., & Lombi, E. (2011). Hair analysis as a biomonitor for toxicology, disease and health status. *Chemical Society Reviews*, *40*(7), 3915–3940. doi: 10.1039/c1cs15021a

Kempson, I. M., & Skinner, W. M. (2005). Tof-sims analysis of elemental distributions in human hair. *Science of the Total Environment*, *338*(3), 213–227. doi: 10.1016/j.scitotenv.2004.07.017

Kempson, I. M., & Skinner, W. M. (2012). A comparison of washing methods for hair mineral analysis: Internal versus external effects. *Biological Trace Element Research*, *150*(1-3), 10–14. doi: 10.1007/s12011-012-9456-z

Kempson, I. M., Skinner, W. M., & Kirkbridge, K. P. (2006). Advanced analysis of metal distributions in human hair. *Environmental Science & Technology*, *40*(10), 3423–3428. doi: 10.1021/es052158v

Langbein, L., Rogers, M. A., Winter, H., Praetzel, S., Beckhaus, U., Rackwitz, H.-R., & Schweizer, J. (1999). The catalog of human hair keratins: I. expression of the nine type i members in the hair follicle. *Journal of Biological Chemistry*, *274*(28), 19874–19884. Retrieved from http://www.jbc.org/content/274/28/19874.abstract doi: 10.1074/jbc.274.28.19874

Lin, K., Xiang, Y., Liu, X., Wu, Z., Bukkens, S. G. F., Tommaseo, M., & Paoletti, M. G. (1999). Metallic elements in hair as a biomarker of human exposure to environmental pollution: A preliminary investigation in hubei province. *Critical Reviews in Plant Sciences*, *18*(3), 417–428. Retrieved from http://www.tandfonline.com/doi/abs/10.1080/07352689991309315 doi: 10.1080/07352689991309315

Mérigoux, C., Briki, F., Sarrot-Reynauld, F., Salomé, M., Fayard, B., Susini, J., & Doucet, J. (2003). Evidence for various calcium sites in human hair shaft revealed by sub-micrometer x-ray fluorescence. *Biochimica et Biophysica Acta*, *1619*(1), 53–58. doi: 10.1016/s0304-4165(02)00441-5

Martin, R. R., Kempson, I. M., Naftel, S. J., & Skinner, W. M. (2005). Preliminary synchrotron analysis of lead in hair from a lead smelter worker. *Chemosphere*, *58*(10), 1385–1390. Retrieved from http://www.sciencedirect.com/science/article/pii/S0045653504008963 doi: 10.1016/j.chemosphere.2004.09.087

Nowak, B., & Chmielnicka, J. (2000). Relationship of lead and cadmium to essential elements in hair, teeth, and nails of environmentally exposed people. *Ecotoxicology and Environmental Safety*, *46*(3), 265–274. Retrieved from http://www.sciencedirect.com/science/article/pii/S0147651300919213 doi: 10.1006/eesa.2000.1921

Patra, R. C., Swarup, D., Naresh, R., Kumar, P., Nandi, D., Shekhar, P., ... Ali, S. L. (2007). Tail hair as an indicator of environmental exposure of cows to lead and cadmium in different industrial areas. *Ecotoxicology and Environmental Safety*, *66*(1), 127–131. Retrieved from http://www.sciencedirect.com/science/article/pii/S0147651306000212 doi: 10.1016/j.ecoenv.2006.01.005

Rendic, D., Holjevic, S., Valkovic, V., Zabel, T. H., & Phillips, G. C. (1976). Trace-element concentrations in human hair measured by proton-induced x-ray emission. *Journal of Investigative Dermatology*, *66*(6), 371–375. doi: 10.1111/1523-1747.ep12482984

Renshaw, G. D., Pounds, C. A., & Pearson, E. F. (1972). Variation in lead concentration along single hairs as measured by non-flame atomic absorption spectrophotometry. *Nature*, *238*(5360), 162–163. doi: 10.1038/238162a0

Robbins, C. (1994). Chemical composition. In *Chemical and physical behavior of human hair* (pp. 55–92). Springer New York. doi: 10.1007/978-1-4757-3898-8_2

Rodushkin, I., & Axelsson, M. D. (2000). Application of double focusing sector field icp-ms for multielemental characterization of human hair and nails. part ii. a study of the inhabitants of northern sweden. *Science of The Total Environment*, *262*(12), 21–36. Retrieved from http://www.sciencedirect.com/science/article/pii/S0048969700005313 doi: 10.1016/S0048-9697(00)00531-3

Rodushkin, I., & Axelsson, M. D. (2003). Application of double focusing sector field icp-ms for multielemental characterization of human hair and nails. part iii. direct analysis by laser ablation. *Science of The Total Environment*, *305*(13), 23–39. Retrieved from http://www.sciencedirect.com/science/article/pii/S0048969702004631 doi: 10.1016/S0048-9697(02)00463-1

Sera, K., Futatsugawa, S., & Murao, S. (2002). Quantitative analysis of untreated hair samples for monitoring human exposure to heavy metals. *Nuclear Instruments and Methods in Physics Research Section B: Beam Interactions with Materials and Atoms*, *189*(14), 174–179. Retrieved from http://www.sciencedirect.com/science/article/pii/S0168583X01010345 doi: 10.1016/S0168-583X(01)01034-5

Smart, K. E., Kilburn, M., Schroeder, M., Martin, B. G., Hawes, C., Marsh, J. M., & Grovenor, C. R. (2009). Copper and calcium uptake in colored hair. *Journal of Cosmetic Science*, *60*(3), 337–45. doi: 10.1111/j.1468-2494.2010.00549_3.x

Sukumar, A., & Subramanian, R. (2007). Relative element levels in the paired samples of scalp hair and fingernails of patients from new delhi. *Science of the Total Environment*, *372*(2-3), 474–479. doi: 10.1016/j.scitotoenv.2006.10.020

Sweileh, J. A. (2003). Sorption of trace metals on human hair and application for cadmium and lead pre-concentration with flame atomic absorption determination. *Analytical and Bioanalytical Chemistry*, *375*(3), 450–455.

Taylor, A. (1986). Usefulness of measurements of trace elements in hair. *Annals of Clinical Biochemistry*, *23*(4), 364–378. doi: 10.1177/000456328602300402

Tipple, B. J., Chau, T., Chesson, L. A., Fernandez, D. P., & Ehleringer, J. R. (2013). Isolation of strontium pools and isotope ratios in modern human hair. *Analytica Chimica Acta*, *798*(0), 64–73. Retrieved from `http://www.sciencedirect.com/science/article/pii/S0003267013011720` doi: 10.1016/j.aca.2013.08.054

Webb, E., White, C., & Longstaffe, F. (2013). Dietary shifting in the nasca region as inferred from the carbon- and nitrogen-isotope compositions of archaeological hair and bone. *Journal of Archaeological Science*, *40*(1), 129–139. doi: 10.1016/j.jas.2012.08.020

Yates, B. C., Espinoza, E. O., & Baker, B. W. (2010). Forensic species identification of elephant (elephantidae) and giraffe (giraffidae) tail hair using light microscopy. *Forensic science, medicine, and pathology*, *6*(3), 165–71. doi: 10.1007/s12024-010-9169-6

Yoshinaga, J., Shibata, Y., & Morita, M. (1993). Trace elements determined along single strands of hair by inductively coupled plasma mass spectrometry. *Clinical Chemistry*, *39*(8), 1650–1655.